J. Fluid Mech. (2024), *vol*. 980, A33, doi:10.1017/jfm.2024.34

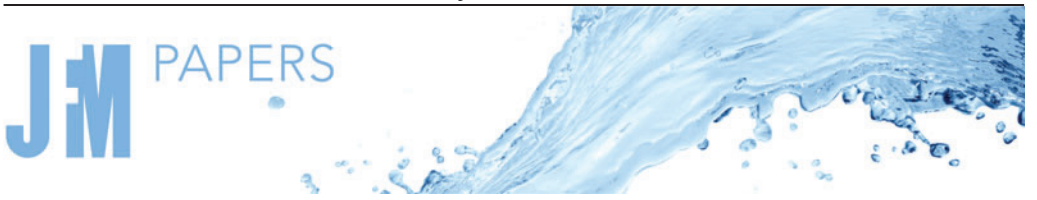

Streamwise dispersion of soluble matter in solvent flowing through a tube

Mingyang Guan[1] **and Guoqian Chen**[1,2,†]

[1]Laboratory of Systems Ecology and Sustainability Science, College of Engineering, Peking University, Beijing 100871, PR China

[2]Macao Environmental Research Institute, Macau University of Science and Technology, Macao 999078, PR China

(Received 14 April 2023; revised 8 November 2023; accepted 1 January 2024)

For the dispersion of soluble matter in solvent flowing through a tube as investigated originally by G.I. Taylor, a streamwise dispersion theory is developed from a Lagrangian perspective for the whole process with multi-scale effects. By means of a convected coordinate system to decouple convection from diffusion, a diffusion-type governing equation is presented to reflect superposable diffusion processes with a multi-scale time-dependent anisotropic diffusivity tensor. A short-time benchmark, complementing the existing Taylor–Aris solution, is obtained to reveal novel statistical and physical features of mean concentration for an initial phase with isotropic molecular diffusion. For long times, effective streamwise diffusion prevails asymptotically corresponding to the overall enhanced diffusion in Taylor's classical theory. By inverse integral expansions of local concentration moments, a general streamwise dispersion model is devised to match the short- and long-time asymptotic solutions. Analytical solutions are provided for most typical cases of point and area sources in a Poiseuille tube flow, predicting persistent long tails and skewed platforms. The theoretical findings are substantiated through Monte Carlo simulations, from the initial release to the Taylor dispersion regime. Asymmetries of concentration distribution in a circular tube are certified as originated from (*a*) initial non-uniformity, (*b*) unidirectional flow convection, and (*c*) non-penetration boundary effect. Peculiar peaks in the concentration cloud, enhanced streamwise dispersivity and asymmetric collective phenomena of concentration distributions are illustrated heuristically and characterised to depict the non-equilibrium dispersion. The streamwise perspective could advance our understanding of macro-transport processes of both passive solutes and active suspensions.

Key words: dispersion

† Email address for correspondence: gqchen@pku.edu.cn

1. Introduction

The problem of dispersion in confined shear flows is a classical textbook subject for physical transport processes and environmental fluid mechanics (Fischer 1973, 1979; Chatwin & Allen 1985). The theoretical study of dispersion stems from two seminal papers of Sir Geoffery Taylor (Taylor 1953, 1954*c*) proposing a longitudinal dispersion equation behind the combined effect of transverse diffusion and streamwise advection, as formulated later more mathematically by Aris (1956). Taylor's dispersion model focuses on an asymptotic distribution of cross-sectional mean concentration for diverse transport phenomena of inorganic salts, natural sediments, waste heat, synthetic organic colloidal species and biological agents (Fischer 1972; Chatwin 1974; Pedley & Kessler 1992), to name just a few. Indeed, research on mechanisms and models associated with Taylor dispersion has not waned; evidence of its continued relevance can be seen in recent studies on soluble matter (Vedel & Bruus 2012; Vedel, Hovad & Bruus 2014; Wu & Chen 2014; Wang & Chen 2016*b*; Taghizadeh, Valdés-Parada & Wood 2020; Chu *et al.* 2021; Wang *et al.* 2022*b*) and self-propelling swimmers (Bearon, Hazel & Thorn 2011; Bearon & Hazel 2015; Jiang & Chen 2021; Fung, Bearon & Hwang 2022; Wang, Jiang & Chen 2022*a*, 2023; Guan *et al.* 2023). The wide-ranging applicability of dispersion encompasses diverse disciplines, from physics to biology and ecology, addressing issues such as cargo transport (Yasa *et al.* 2018), algae blooms (Durham, Kessler & Stocker 2009; Durham *et al.* 2013), bed-load transport (Wu, Furbish & Foufoula-Georgiou 2020) and surface transient storage (Wang & Cirpka 2021). Taylor dispersion holds significance in emerging technological processes, such as those explored in diffusiophoresis (Chu *et al.* 2021; Alessio *et al.* 2022) and trapping (Jiang & Chen 2021; Wang *et al.* 2022*a*), as well as hydrodynamic focusing (Kessler 1985; Guan *et al.* 2023).

For unidirectional ambient flows, Taylor's original model holds thanks to conditions of the predominant longitudinal convection effect over that of molecular diffusion and a sufficiently long time to reach the dispersion regime compared to the characteristic diffusion scale for the thorough mixing of a solute over the cross-section (Taylor 1954*a*; Chatwin & Allen 1985). Taylor's simple derivation was praised as 'a display of the sort of brilliance we can only admire' by Fischer (1976), which indicates a need to revisit and explore the nature of the dispersion process. Moreover, a general procedure for dealing with the convection–diffusion problem is not available, and no general particular solution of transient dispersion can be found (Fischer 1979). In this paper, we will elucidate the dispersion of soluble matter with a convected coordinate transformation applying to the convection–diffusion equation, to extend intensively Taylor's dispersion model from a Lagrangian perspective.

In a numerical simulation of dispersion, Sullivan (1971) obtained the statistical properties of concentration distribution with the random walk method, and identified three stages of transient streamwise dispersion. The skewed distributions reported are consistent with the laboratory measurements of Taylor (1954*b*) and Elder (1959). From the perspective of moment statistics (Aris 1956) in the streamwise direction, Gill (1967) started with series solutions of unsteady convective diffusion model equation as an approximation to the fundamental convection–diffusion dynamical system, of which the time-dependent diffusivity received the logical criticism (Taylor 1959) and supportive correspondence of Taylor (Gill, Sankarasubramanian & Taylor 1970). With asymptotic long-time expansions subject to the superposition principle, Chatwin (1970) devised an equivalent Edgeworth series of mean concentration distribution to account for the asymmetric physical structures caused by diffusion and boundary conditions. However, these contributions are limited to the description of mean concentration distribution from an area source for asymptotically

long times. It is clear that we lack a general theory for transient dispersion – an extension to Taylor's.

The above discussion is intimately related to the physical structures and dispersion mechanisms. Under the simultaneous effect of both variations of velocity profile and molecular diffusion, the overall dispersion process undergoes different regimes with rich balance mechanisms. Through scaling laws and numerical analyses, researchers have explored extensively different mechanisms corresponding to each dispersion regime (Lighthill 1966; Chatwin 1970; Young & Jones 1991; Phillips & Kaye 1997; Houseworth 1984; Latini & Bernoff 2001). Houseworth (1984) made a strategic overview of instantaneous point source releases focusing on the transitional stage, conducting scale analysis on the tube axis and near the boundary wall, respectively. Latini & Bernoff (2001) first depict three transient dispersion regimes by scaling analysis from a point source discharge at the tube axis, namely diffusive, anomalous and classical Taylor regimes. They developed a compact derivation for the head and tail distributions of mean concentration, respectively, aiming chiefly at the anomalous regime and ignoring the boundary wall. Before and after a solute approaches the wall, there exists a prominent transition of the concentration profiles. Therefore, the anomalous regime should inherently give birth to more interesting phenomena. In the light of streamwise dispersion theory, we will reveal and predict richer physical structures of different dispersion regimes with an inverse integral expansion method, verified numerically with Monte Carlo simulations. Three time scales will be deduced naturally by a convection transformation from a first principle, and predominant structures will be clarified for each transport regime.

The inevitability of non-Gaussian distributions leads to two different attempts historically: (*a*) the approach to a normal distribution, and (*b*) the evolution from the initial solution. The basic physics of Taylor dispersion is general in both cases, even though direct Gaussian approximations might fail during the transitional stage. A significant advance has been achieved by Smith (1982*b*) for a Gaussian approximation along the streamline with a uniform area source. His approximation stems from the short-time approximated source solution of Saffman (1960) and the long-time Gaussian solution of Taylor's dispersion model. Note that the adopted short-time benchmark is indeed not an exact description directly from the convection–diffusion equation. What disappointed Smith is that his one-term Gaussian approximation of the natural inferences from approximate solutions seems unable to reproduce the asymmetric hallmarks quantitatively. Smith (1981, 1982*a*) later devised a promising model equation with explicit source terms, i.e. a delay–diffusion equation, with the understanding that the transient dispersion is a gradual process dependent on earlier times. Li (2018) extended the Taylor–Aris method to analyse transverse concentration. Smith (1981, 1982*b*) and Li (2018) succeeded qualitatively in producing an essential asymmetric profile. Nevertheless, quantitatively satisfactory modelling of such asymmetric structures and other inherent features during transitional regimes remains challenging. There is a need to develop some more general models to catch the hallmarks of transient dispersion.

In this paper, the dispersion process is explored rigorously in terms of both basic mechanisms and analytical solutions, with case studies on fundamental source releases in a Poiseuille tube flow, where results are readily extendable to circumstances in other confined flows. The paper is structured as follows. In § 2, we undertake a thorough review of the historical development of dispersion models. Concurrently, we highlight a notable gap in the current dispersion theory concerning the absence of transient streamwise features, and elucidate the pertinence of our proposed approach with a wide

spectrum of applications in the contemporary context. Revisiting the classical dispersion problem in § 3, we will devise and apply a convection transformation from a first principle, and provide a short-time particular solution from the central point discharge for the transformed convection–diffusion equation. A streamwise theory of dispersion is formulated that dispenses with Taylor's assumptions, matching the accurate statistics of concentration distribution. The streamwise dispersion theory would be demonstrated in § 4 to reveal new physical structures of transient dispersion and to certify the basic origins of asymmetries. In § 5, we will formulate and examine a streamwise dispersion model for typical area and point sources. The streamwise solution reduces to the benchmark obtained rigorously for asymptotically short times and Taylor's particular solution for asymptotically long times, while also behaving satisfactorily for the transitional dispersion regimes. Finally, § 6 concludes.

2. Literature review

With particular attention paid to the asymptotic behaviour of moment statistics, we emphasise that the method of concentration moment is general to depict real-time streamwise information of transient dispersion. However, due to related computational complexities, only the incorporation of coarse-grained moment statistics other than exact streamwise information into the distribution of concentration was achieved for almost all the existing dispersion models. Taylor's original theory applies only when a solute cloud disperses longitudinally with an overall effective diffusion coefficient. In turn, this method of evaluating the dispersion coefficient has been applied widely and extended for various flow structures (Yasuda 1984; Chikwendu & Ojiakor 1985; Chikwendu 1986; Haber & Mauri 1988; Guo & Chen 2022). The eventual Gaussian form of solution of transient dispersion problems inspired many scholars to develop series expansions based on moment derivatives. The procedure is an extension of Taylor's dispersion model, and yields an improved high-order description on the asymmetries of mean concentration. Given the difficulty in solving time-dependent functions beyond the first three orders (Gill 1967), an approach by Wang & Chen (2016*a*, 2017) involved the utilisation of the method of moments to approximate the coefficients within Gill's model. Subsequently, Jiang & Chen (2018) further solved the model analytically, linking it to macroscopic phenomenological transport coefficients, focusing specifically on the third- and fourth-order cumulants (skewness and kurtosis). These results are satisfactory to describe the approach of an initial area source to the normality of the concentration distribution, specifically for times greater than $0.5a^{*2}/D^*$ (Chatwin 1970), where D^* is the molecular diffusion coefficient, and a^* is the radius of the tube. Although with an improved quantitative description of the mean concentration for some later transitional phases before asymptotics, this kind of monolithic technological endeavour hardly furnishes conceptual insights into the overall physical processes (Brenner & Edwards 1993).

With abundant information about asymptotic Taylor dispersion, efforts have been pursued to study the early-time dispersion behaviour. Lighthill (1966) attempted to establish a complementary theory towards the Taylor dispersion model as focused on the initial evolution of diffusion at times less than $0.1a^{*2}/D^*$. By neglecting the axial diffusion and boundary conditions, Lighthill gave an approximation of the initial concentration in an infinite plane, and specified a time scale when the discontinuity is removed by radial diffusion. Chatwin (1976) commented on Lighthill's solution that the approximation is indeed dominant for the pre-asymptotic stage rather than the initial stage. Lighthill's exact solution should thus be regarded as an improvement upon the

illustrative yet non-physical pure advection model of Taylor (1953) that totally ignores molecular diffusion. Chatwin (1976) then extended Lighthill's solution to include the effect of axial diffusion accounting for the anomalous stage. However, the practical use of this extended result is very limited for the transitional stage due to the restrictions of the direct temporal expansion (by $t^{-1/2}$) and infinite plane assumption, as verified numerically by Houseworth (1984). With the intuition that the initial transport mechanism might be a direct axial diffusion process, Saffman (1960) displayed an approximate source solution in the Gaussian form moving at the mean flow speed for the initial concentration. Further, Chatwin (1977) discussed Saffman's solution with the superposition principle for different source releases in infinite space, and depicted the boundary condition with the image method. Although the application of this solution is limited, rather, to an early stage (Chatwin 1977; Dewey & Sullivan 1982; Houseworth 1984), the attempt reflected the physical importance of fundamental source solutions, and gave formally correct approximations of dispersion coefficients and concentration distributions within the early stage.

Vigorous endeavours have been undertaken in the quest for the earlier validity of dispersion approaches extending into the transitional phase encompassing anomalous and pre-asymptotic regimes, all of which pose formidable challenges. Based on the asymptotic analysis, Chatwin (1972) explained the deviation of experimental observations from tilted Gaussian curves by further obtaining the cumulants of concentration distribution. Wu & Chen (2014) examined the approach of transverse uniformity in concentration distribution using a homogenisation technique. As revealed, the rate to approach transverse uniformity is considerably slower than that to approach streamwise normality. Gill *et al.* (1970) continued searching for an exact solution of the convection–diffusion model equation with unsteady coefficients. Frankel & Brenner (1989) generalised the original Taylor dispersion theory for non-unidirectional transport processes in multiple media with a constant set of coefficients independent of space and time. The wavenumber expansion based on the centre manifold theorem by Mercer & Roberts (1990) is effective equivalently to Smith (1981) but algebraically simpler, as reviewed by Young & Jones (1991) in detail. Generally, these efforts captured parts of exact moment statistics by devising approximations or model equations for the convection–diffusion problem, whilst some solutions could be pursued only numerically.

With the prompt development of dispersion models, unifying descriptions applicable for all times necessarily attract greatest attention. Based on the fundamental solution by Townsend & Taylor (1951) in a flow field with a linear velocity profile, Foister & van de Ven (1980) discussed the diffusion of Brownian particles with perturbation expansions in general linear flows and unbounded Poiseuille flows. Pasmanter (1985) further gave some explicit approximations for the convection–diffusion equation with systematic Lie algebra techniques in an infinite plane, for some classical linear and parabolic velocity fields. For bounded Poiseuille flow, Houseworth (1984) examined numerically the evolution of residence time distribution with an extended Monte Carlo method. Detailed features of each dispersion regime are present for the area and point sources. Stokes & Barton (1990) applied integral transforms, and their numerical procedures gave a precise description of mean concentration distribution for area source releases with an infinite Péclet number. Phillips & Kaye (1997) then extended the ideas of Stokes & Barton (1990), and derived an expansion in the form of the product of Laguerre and Gaussian polynomials, recovering Lighthill's solution with a leading-order correction. Their approximations could describe effectively the peaking head of concentration distribution during the anomalous regime. Recently, Taghizadeh *et al.* (2020) focused on the pre-asymptotic dispersion regime and

illustrated the challenge in numerical simulation of the spreading of soluble matter at early times, addressing the need for more vigorous analytical exploration. Nonetheless, the modelling and prediction of asymmetric physical structures concerning streamwise dispersivity, as well as transverse and mean concentration distribution under fundamental initial conditions, continue to represent an unresolved classical challenge, not only from the perspective of physical mechanisms, but also for the lack of conceptual framework and analytical approaches.

The recent necessity of dispersion research is underscored by the expanding breadth of deepening theoretical explorations and ongoing investigation of novel phenomena from both natural and artificial scopes. Urgency arises from the escalating prevalence of practical applications and the unexplored frontiers of new mechanisms. The dispersion analysis has undergone substantial extensions (Brenner & Edwards 1993; Bello, Rezzonico & Righetti 1994; Biswas & Sen 2007; Jiang & Chen 2019; Wu *et al.* 2020, 2023; Nakad *et al.* 2021; Wang & Cirpka 2021; Vilquin *et al.* 2023). Particle loss resulting from either particle absorption or chemical reactions can alter significantly the probability distributions, thereby introducing intricacies into dispersion models (Zhang, Hesse & Wang 2017; Jiang *et al.* 2022; Vilquin *et al.* 2023). Activity and reactivity could play a critical role in Taylor dispersion, particularly in the context of chemistry and life sciences (Hong *et al.* 2020; Deleanu *et al.* 2021; Jiang & Chen 2021; Moser & Baker 2021; Guan *et al.* 2023; Wang *et al.* 2023). In addition, comprehending the mechanisms beneath these intriguing phenomena and applications requires a model-based approach. Commencing from the fundamental first principles, it is imperative to construct a mechanistic model through empirical observations. The model, in turn, will serve as a benchmark for practical experimental measurements and numerical simulations (Li & Tang 2009; Durham *et al.* 2013; Rusconi, Guasto & Stocker 2014; Barry *et al.* 2015; Ezhilan & Saintillan 2015; Sokolov & Aranson 2016). We hope that the streamwise perspective can offer an exemplary framework for the theoretical analysis of active suspensions (Jiang & Chen 2019; Guan *et al.* 2023), analogous to its application for passive particles (Guo, Jiang & Chen 2020; Guo & Chen 2022).

The preceding literature review leads us to the following long-standing questions of basic research interest.

(i) What is the exact diffusion-type formulation of streamwise dispersion?
(ii) How can we predict the transient physical structures of concentration distribution?

To resolve these issues, we now limit our attention to the classical dispersion of passive solutes in a steady parallel flow (e.g. pressure-driven Poiseuille tube flow) such that analytical approaches of the developed streamwise dispersion theory and model are feasible. Based on the above discussion, two significant conclusions are drawn: (*a*) a modified diffusion-type distribution of transient dispersion must come from real-time streamwise considerations rather than coarse-grained input; (*b*) moment statistics are particularly helpful to obtain such transient streamwise features. The answer to the first question will be provided inherently by our developed streamwise theory, of which the generality should open the door to the extensions of existing dispersion and transport models of passive and active particles. Based on exact particular solutions from first principles, we will derive analytically practicable solutions of the developed streamwise dispersion model. This will involve comprehensive utilisation of transient streamwise information obtained from moment statistics, aimed at addressing the second concern.

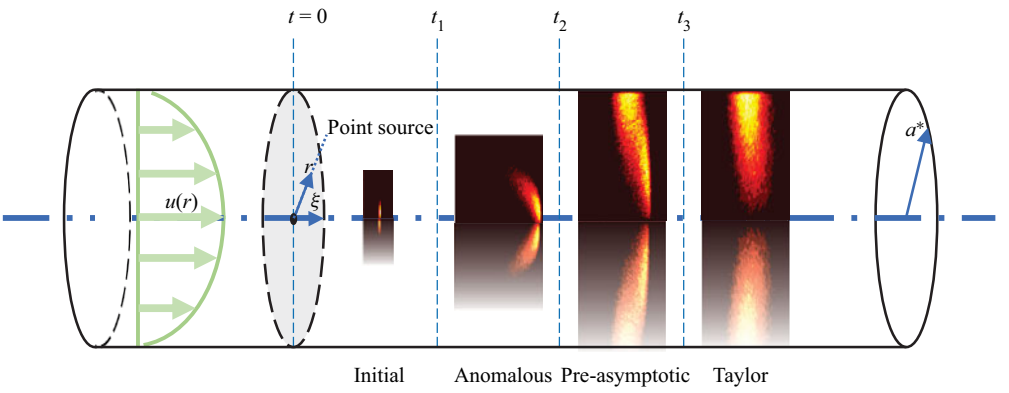

Figure 1. Illustration of transient Taylor dispersion for a central point release in a Poiseuille tube flow. Note that the illustrated concentration distribution is averaged azimuthally.

3. Streamwise dispersion theory

3.1. *Convected coordinate based diffusion formulation*

We revisit the classical axisymmetrical problem of a solute cloud with total mass Q^* dispersing in a steady parallel flow. Consider the classical Poiseuille tube flow with mean flow velocity u in an insulated long tube, as shown in figure 1. In the cylindrical coordinate system (where ξ denotes the axial coordinate, and r is the radial coordinate) at time t, the convection–diffusion equation of concentration C reads (Taylor 1953; Aris 1956; Chatwin 1970; Gill 1971)

$$\frac{\partial C}{\partial t} + Pe\, u(r)\frac{\partial C}{\partial \xi} = \frac{\partial^2 C}{\partial \xi^2} + \frac{1}{r}\frac{\partial}{\partial r}\left(r\frac{\partial C}{\partial r}\right). \tag{3.1}$$

Dimensionless variables above are normalised as

$$C = \frac{C^* a^{*3}}{Q^*}, \quad t = \frac{t^* D^*}{a^{*2}}, \quad Pe = \frac{U^* a^*}{D^*}, \quad u = \frac{u^*}{U^*}, \quad \xi = \frac{\xi^*}{a^*}, \quad r = \frac{r^*}{a^*}, \tag{3.2a–f}$$

where C^* is the dimensional concentration, a^* is the radius of the tube, t^* is the time, D^* is the mean diffusivity, Pe is the Péclet number, u^* is the flow velocity, U^* is the mean flow velocity, ξ^* is the axial coordinate, and r^* is the radial coordinate. The initial condition reads as

$$C|_{t=0} = \mathcal{C}^0(\xi, r), \tag{3.3}$$

where $\mathcal{C}^0$ is the initial concentration distribution corresponding to

$$\int_{-\infty}^{\infty} \mathrm{d}\xi \int_0^1 2r\,\mathrm{d}r\,\mathcal{C}^0 = 1. \tag{3.4}$$

Boundary conditions are employed as

$$C \to 0 \quad \text{as } |\xi| \to \infty, \tag{3.5}$$

$$\left.\frac{\partial C}{\partial r}\right|_{r=0} = \left.\frac{\partial C}{\partial r}\right|_{r=1} = 0. \tag{3.6}$$

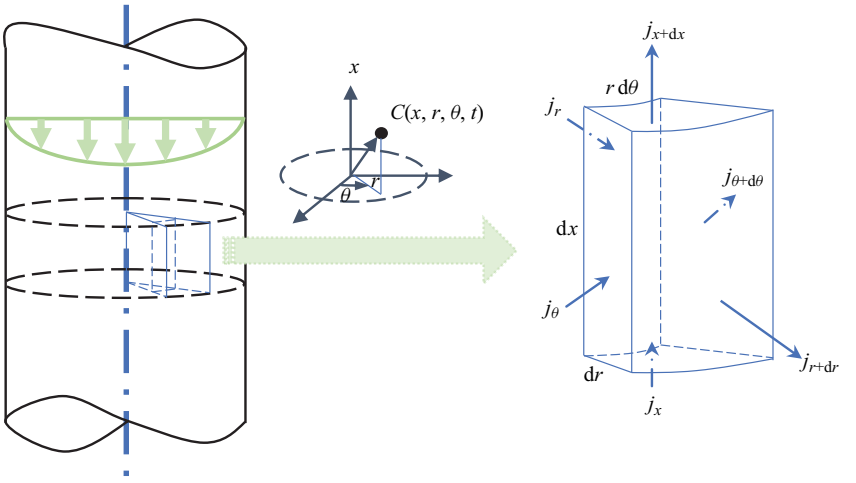

Figure 2. Convection–diffusion analysis in the ordinary cylindrical coordinates (ξ, r, θ) and differential control volume $\mathrm{d}x \times r\,\mathrm{d}\theta \times \mathrm{d}r$, in the form of a pure diffusion equation for the convected system (x, r, θ).

As practised widely in continuum mechanics (Crank 1975; Hahn & Özişik 2012), a convected coordinate system that moves with the fluid particle along each streamline is introduced,

$$x = \xi - Pe\, u(r)\, t, \tag{3.7}$$

for a convection transformation to decouple convection from the diffusion effect. A Poiseuille tube flow velocity hereafter should be substituted as $u(r) = 1 - r^2$. Notice that as an original case in scalar transport, an upwind transformation has been devised for the construction of compact finite difference schemes for the convective–diffusion equation by Chen & Gao (1991) and Chen, Gao & Yang (1993). Substituting this transformation (3.7) into the normalised convection–diffusion equation with the chain rule yields a diffusion equation

$$\frac{\partial C}{\partial t} = \nabla \cdot (\boldsymbol{D} \nabla C), \tag{3.8}$$

with the divergence operator

$$\nabla \cdot \boldsymbol{g} = \frac{\partial g_x}{\partial x} + \frac{1}{r}\frac{\partial (r g_r)}{\partial r}, \tag{3.9}$$

where g_x and g_r are the axial and radial components of $\boldsymbol{g}$, respectively. This diffusion-type formulation can be obtained from a first principle with reference to figure 2.

The rate of transfer of diffusing matter through unit area of a cross-section is given by Fick's law as

$$\boldsymbol{j} = -\nabla C, \tag{3.10}$$

where the gradient operator is

$$\nabla f(x, r) \equiv \begin{bmatrix} \dfrac{\partial f(x, r)}{\partial x} \\ \dfrac{\partial f(x, r)}{\partial r} \end{bmatrix}, \tag{3.11}$$

and using the chain rule, the concentration flux components in the axial and radial directions are, respectively,

$$j_x = -\frac{\partial C}{\partial x}, \quad j_r = -\left(2\,Pe\,tr\,\frac{\partial C}{\partial x} + \frac{\partial C}{\partial r}\right). \tag{3.12a,b}$$

In the convected coordinate system, we now calculate each component normal to the section of the differential control volume. The rate of increase of dispersing matter through the inward section is given by

$$r\,\mathrm{d}\theta\left(j_r - \frac{1}{2}\,\frac{\partial j_r}{\partial r}\,\mathrm{d}r\,\mathrm{d}x - Pe\,tr\,\frac{\partial j_r}{\partial x}\,\mathrm{d}x\,\mathrm{d}r\right), \tag{3.13}$$

and the rate of loss through the outward section is

$$r\,\mathrm{d}\theta\left(j_r + \frac{1}{2}\,\frac{\partial j_r}{\partial r}\,\mathrm{d}r\,\mathrm{d}x + Pe\,tr\,\frac{\partial j_r}{\partial x}\,\mathrm{d}x\,\mathrm{d}r\right). \tag{3.14}$$

Thus the total contribution to the rate of increase of dispersing matter in the element between these two faces is equal to

$$-r\,\mathrm{d}\theta\,\mathrm{d}x\,\frac{\partial j_r}{\partial r}\,\mathrm{d}r - 2\,Pe\,tr^2\,\mathrm{d}\theta\,\mathrm{d}r\,\frac{\partial j_r}{\partial x}\,\mathrm{d}x. \tag{3.15}$$

Similarly, for the longitudinal faces we obtain

$$-r\,\mathrm{d}\theta\,\mathrm{d}r\,\frac{\partial j_x}{\partial x}\,\mathrm{d}x. \tag{3.16}$$

Note that the rate of change of dispersing matter in the control volume is

$$r\,\mathrm{d}\theta\,\mathrm{d}x\,\mathrm{d}r\,\frac{\partial C}{\partial t}. \tag{3.17}$$

Combining the above contributions, the conservation law requires for the axisymmetrical case

$$\frac{\partial C}{\partial t} + \frac{\partial j_r}{\partial r} + 2\,Pe\,tr\,\frac{\partial j_r}{\partial x} + \frac{\partial j_x}{\partial x} = 0. \tag{3.18}$$

Then the substitution of (3.12*a*,*b*) into (3.18) results in (3.8). Accordingly, the equivalent diffusivity tensor in (3.8) is obtained as

$$\boldsymbol{D} = \begin{bmatrix} 1 + (Pe\,t)^2\,|\nabla u|^2 & -Pe\,t\,\nabla u \\ -Pe\,t\,\nabla u & 1 \end{bmatrix}. \tag{3.19}$$

The convection transformation deduces naturally three time scales with respect to the product of the Péclet number and dimensionless time, with a partition of $\boldsymbol{D}$

$$\boldsymbol{D} = \boldsymbol{D}^{(\boldsymbol{O})} + Pe\,t\boldsymbol{D}^{(\boldsymbol{C})} + (Pe\,t)^2\boldsymbol{D}^{(\boldsymbol{E})}, \tag{3.20}$$

wherein

$$\boldsymbol{D}^{(\boldsymbol{O})} = \begin{bmatrix} 1 & 0 \\ 0 & 1 \end{bmatrix}, \quad \boldsymbol{D}^{(\boldsymbol{C})} = \begin{bmatrix} 0 & \nabla u \\ \nabla u & 0 \end{bmatrix}, \quad \boldsymbol{D}^{(\boldsymbol{E})} = \begin{bmatrix} |\nabla u|^2 & 0 \\ 0 & 0 \end{bmatrix}. \tag{3.21a–c}$$

The first tensor $\boldsymbol{D}^{(\boldsymbol{O})}$ represents the isotropic molecular diffusion of soluble matter; the second tensor $\boldsymbol{D}^{(\boldsymbol{C})}$ denotes a cross-enhancement due to the velocity shear; and the

third tensor $\boldsymbol{D}^{(\boldsymbol{E})}$ quantifies a dispersal enhancement along the axial direction. With the decomposition, (3.8) is detailed as

$$\frac{\partial C}{\partial t} = \nabla \cdot (\boldsymbol{D}^{(\boldsymbol{O})} \nabla C) + Pe\, t\, \nabla \cdot (\boldsymbol{D}^{(\boldsymbol{C})} \nabla C) + (Pe\, t)^2\, \nabla \cdot (\boldsymbol{D}^{(\boldsymbol{E})} \nabla C). \tag{3.22}$$

For a given Péclet number, at a short time we retain a conventional isotropic diffusion equation,

$$\frac{\partial C}{\partial t} = \frac{\partial^2 C}{\partial x^2} + \frac{1}{r}\frac{\partial}{\partial r}\left(r\frac{\partial C}{\partial r}\right), \tag{3.23}$$

and for long times, we obtain a one-dimensional streamwise diffusion equation,

$$\frac{\partial C}{\partial t} = 4r^2\, Pe^2\, t^2\, \frac{\partial^2 C}{\partial x^2}, \tag{3.24}$$

corresponding to the one-dimensional longitudinal diffusion equation for the transverse mean concentration in Taylor's overall dispersion model.

3.2. *Taylor's dispersion model and its extensions*

A solution of Taylor's form for asymptotically long time can be inferred promptly from (3.24). Before deriving a short-time particular solution with the streamwise theory of transient dispersion, we would like to first explain the nature of the model solution by Taylor (1953) and some theoretical generalisations since then.

Consistent with Taylor (1953), Aris (1956), Chatwin (1970) and Gill (1971), we introduce a longitudinal coordinate $x' = \xi - Pe\,\bar{U}t$ at the speed of mean flow velocity $\bar{U} \equiv \int_0^1 u(r)\, 2r\, \mathrm{d}r$, for comparison with the classical theoretical results. In all figures hereafter, a normalised set of $(\bar{C}\, Pe, x'/Pe)$ is adopted. In Taylor's fashion, the convection–diffusion problem can be characterised by a one-dimensional enhanced diffusion equation of mean concentration $\bar{C} \equiv \int_0^1 C\, 2r\, \mathrm{d}r$, well known as the Taylor dispersion model, as

$$\frac{\partial \bar{C}}{\partial t} = K_2 \frac{\partial^2 \bar{C}}{\partial x'^2}. \tag{3.25}$$

To determine the coefficient of diffusion K_2, Taylor (1954*a*) assumed that the concentration can be obtained with a Taylor expansion in the vicinity of mean concentration as

$$C = \bar{C} + \sum_{n=1}^{2} K_n(r)\, \frac{\partial^n \bar{C}}{\partial x'^n}. \tag{3.26}$$

By finding a general solution for the radial diffusion equation, he determined K_1. The second-order concentration gradient can be regarded as a small variation in $\partial C/\partial x'$. Substitution of (3.26) into a reduced convection–diffusion equation yields K_2. By analogy with Taylor's manipulation, Gill proposed the transient dispersion model (Gill 1967, communicated by Taylor), as

$$C = \bar{C} + \sum_{n=1}^{\infty} f_n(t, r)\, \frac{\partial^n \bar{C}}{\partial x'^n}, \tag{3.27}$$

which includes Taylor's model as a special case. Jiang & Chen (2018) solved Gill's transient dispersion model by a systematic analytical procedure. The most effective and

prevalent approach to solving the macro-scale equation is expressed in the form of a Kramers–Moyal expansion, i.e. an infinite series of spatial derivatives of concentration. Several successful attempts have been carried out by Chatwin (1970), Gill (1971), Smith (1982*b*) and others.

Inspired by (3.22), it is time to reflect on the extensions of Taylor dispersion and generalise the implications to transient dispersion. Taylor (1953) assumed that the dispersion of a solute relative to the coordinate system moving with the mean flow speed could be predicted by an effective one-dimensional diffusion equation. From a first principle, we show by a convection transformation with the streamwise speed of flow in contrast to Taylor (1954*a*): 'the combined effect of longitudinal convection and radial molecular diffusion is to give rise to a transfer across planes which move with the mean speed of flow', which 'would only be likely to be valid when the time necessary for a radial variation in concentration to die down owing to radial diffusion was much shorter than the time necessary for an appreciable change in concentration to occur through longitudinal convection'. Furthermore, it is clear from (3.22) that the dispersion driven by convection and diffusion is indeed a diffusion process without arbitrary assumptions as perceived from a streamwise convected coordinate system. A partition of the equivalent diffusivity tensor, with respect to three time scales, shows that the components are anisotropic in space and nonlinear with time. The anisotropy and nonlinearity that complicate the dispersion process are due to the cross-shear effect and axial dispersal enhancement from a convected coordinate. As a result, Gaussian approximations are broadly pursued to reproduce the exact transient dispersion, although no conceptual conclusion has been reached on the matter.

3.3. *Short-time particular solution*

For an instantaneous release as symbolised by an axisymmetrical Dirac delta function for the initial concentration distribution, at small times the solution for (3.23) promptly reads

$$C = \frac{2\pi}{16\pi^{3/2}t^{3/2}} \exp\left\{-\frac{[\xi - Pe\,(1-r^2)t]^2 + (r-r_0)^2}{4t}\right\} \tag{3.28}$$

for a source released at $\xi = 0$, $r = r_0$ in a distance away from the wall. Note that for a small time, there is actually no effect of the boundary wall for an initial central point release of soluble matter, so that the solute disperses as if it were in infinite space from a convected perspective. This short-time particular solution (3.28) applies to instants just after the discharge and implies that the concentration distribution asymptotes to a tilted Gaussian form viewing from each fluid particle. In the Eulerian description moving at the mean flow speed, a long-tailed distribution should be predicted rather than the normal distribution as predicted by Saffman (1960) and Smith (1982*b*). Therefore, our fundamental source solution derived for the initial stage is essentially different from previous well-established approximations. The solutions of initial axial Gaussian type sources, area sources and other non-uniform sources (e.g. initial conditions adopted in Abbott *et al.* 1984; Gekle 2017; Taghizadeh *et al.* 2020) can also be obtained with the superposition of the Green function from the solution of point sources directly, though the solutions from the Gaussian sources or area sources obtained in this manner would be physically meaningless without accounting for the interactions between soluble matter and the boundary. This solution works exactly at very short times when the majority of a solute has not approached the wall, in contrast to Saffman's approximation, which is true only for sufficiently small distance away from the centre in an infinite medium. The solution of Lighthill (1966)

simply takes the conventional assumption in the dispersion analysis that the longitudinal diffusion can be neglected as compared to the convection effect. This condition is not realistic and even contrary to the inherent characteristics of the very initial phase when longitudinal diffusion can be dominant over convection upon instantaneous release of the source. Complexity in his solution results from this non-physical assumption, which is indeed valid for the anomalous regime (Chatwin 1976) rather than the initial stage as declared. In contrast, the straightforward procedure presented in this section indicates the accuracy of (3.28) as a particular solution with physically reasonable approximations, and gives us conceptual insights that the dispersing solute in unsteady parallel flows is actually subject to the equivalent diffusion equations viewed from a convected coordinate system, corresponding to three scales specified by a product of the Péclet number and diffusive time.

For larger times in the initial phase when the solute cloud may appear in the zone near the wall, the boundary restrictions can be released to a first-order approximation by the method of image. When an imaged source is introduced to make the resulting concentration symmetric about the tangent of the tube boundary, the radial derivative of concentration becomes zero, exactly as required by the boundary conditions. From the reduced governing equation (3.1), the axial symmetry and uniqueness of the unit source solution guarantee the effectiveness of the image method as if it were applied to an infinite plane. An image method is applied to account for the reflective boundary condition as

$$C = \frac{2\pi}{16\pi^{3/2}t^{3/2}} \exp\left\{-\frac{[\xi - Pe\,(1-r^2)t]^2 + (r-r_0)^2}{4t}\right\} + \frac{2\pi}{16\pi^{3/2}t^{3/2}} \exp\left\{-\frac{[\xi - Pe\,(1-(r-2+r_0)^2)t]^2 + (r-2+r_0)^2}{4t}\right\}. \tag{3.29}$$

Interestingly, the unified short-time solution (3.29) shows wide adaptability up to $t \sim 0.1$, as shown in figure 3(*d*), compared with Monte Carlo simulation results for characteristic dispersion regimes, where numerical procedures are detailed in § 1 of the supplementary material available at https://doi.org/10.1017/jfm.2024.34. This time scale characterises the initial dispersion regime, almost reaching the lower bound of the applicable time limit of existing extended dispersion models.

The distinctive characteristics of the initial regime are symmetric Gaussian profiles when molecular diffusion is predominant over axial convection, as shown in figure 3(*a*). Physically, the convection transformation represents a streamwise perspective viewing from fluid particles. In such a convected coordinate system, a solute experiences pure diffusion within the initial stage, axially and radially, in a highly symmetric manner similar to the Taylor regime. When the velocity shear dominates axial diffusion, unidirectional convective distortion of the flow field breaks the symmetry and flushes the peaks of mean concentration distribution downstream within the anomalous regime. The head and tail of the concentration profiles are unique features for the transient dispersion, as shown in figures 3(*b–d*). Latini & Bernoff (2001) deduced head and tail approximations for this stage, describing the distortion of the mean concentration profile, respectively. In contrast, the present particular solution gives a compact and precise description of this highly skewed shape of the distribution with lesser substantial error. On the whole, the short-time particular solution (3.29) gives satisfactorily quantitative predictions and reveals new physical structures, complementary to Taylor's long-time solution.

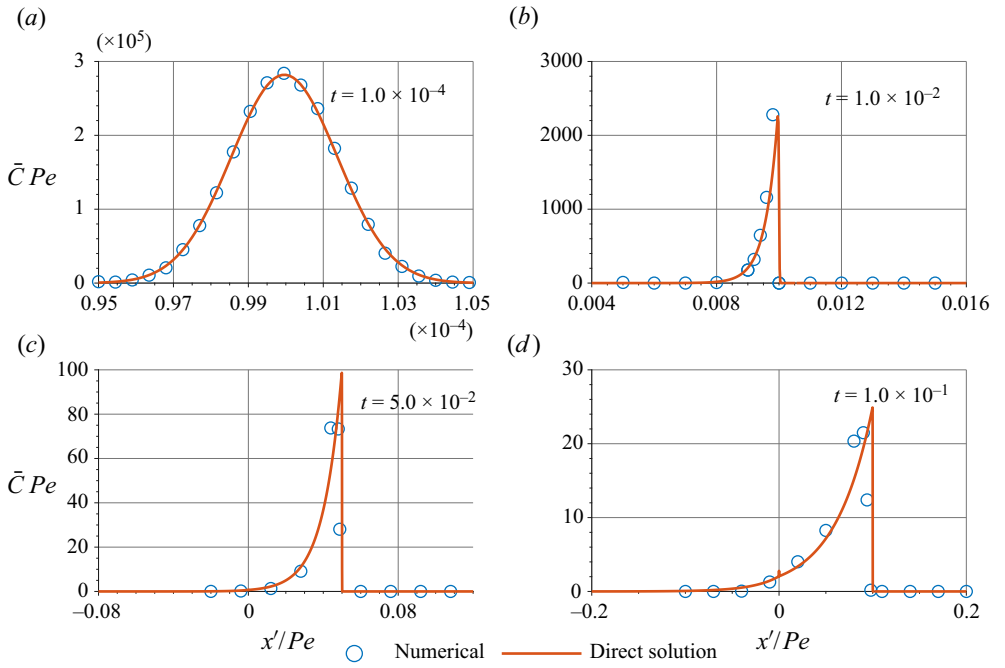

Figure 3. Mean concentration distribution in a Poiseuille tube flow predicted by the short-time particular solution (3.29) compared with the Monte Carlo simulation at times (*a*) $t = 1.0 \times 10^{-4}$, (*b*) $t = 1.0 \times 10^{-2}$, (*c*) $t = 5.0 \times 10^{-2}$, and (*d*) $t = 1.0 \times 10^{-1}$, in Taylor's moving coordinate system. Common parameters are $Pe = 10\,000$ and $r_0 = 0$.

4. Physical structures and origins of asymmetric concentration distribution

4.1. *Implications of physical structures from diffusion flux vectors*

To better understand the implications of the physical structures, we resort to the diffusion flux vector in the convected coordinate system as

$$\boldsymbol{j} = \begin{bmatrix} -(1 + 4\,Pe^2\,t^2 r^2)\,\dfrac{\partial C}{\partial x} - 2\,Pe\,tr\,\dfrac{\partial C}{\partial r} \\ -\dfrac{\partial C}{\partial r} - 2\,Pe\,tr\,\dfrac{\partial C}{\partial x} \end{bmatrix}. \tag{4.1}$$

This expression lends the ground for two observations. The first is that the diffusion in the axial direction is enhanced by the velocity shear, with the extent of enhancement quantified by $4\,Pe^2\,t^2 r^2$. This axial enhancement due to the shear is represented by $\boldsymbol{D}^{(\boldsymbol{E})}$. Second, the diffusion in the axial direction is translated into the radial gradient flux with the extent of enhancement quantified by $2\,Pe\,tr$. This cross-shear enhancement is represented by $\boldsymbol{D}^{(\boldsymbol{C})}$.

The vector (4.1) is heuristic to analyse the original convection–diffusion equation from a Lagrangian view. Enhanced effects are directly proportional to the magnitude of the velocity gradient, and the duration of dispersion also positively correlates with the enhanced effects. The shear varies throughout the flow domain, and these effects are anisotropic and inhomogeneous in the prescribed flow domain at different times. Further, there must be a predefined sub-region for a solute to demonstrate a preference for release positions, leading to an expedited dispersion process, provided that the velocity profile and observation time remain unchanged.

Based on the above analysis, we exemplify a circular ribbon of a solute in a classical Poiseuille tube flow, given that the ribbon is thin in the radial direction and narrow in the axial direction, being released exactly near the tube wall ($r_0 \sim 1$) at $t = 0$. The Eulerian non-penetration boundary condition at the wall ($\partial C/\partial r = 0$) in the convected coordinate becomes a no-flux condition ($\partial C/\partial r + 2\,Pe\,tr\,\partial C/\partial x = 0$) at $r = 1$.

The intrinsic feature of Poiseuille tube flow determines that $|\nabla u|$ is largest at the wall. Remarkable cross and enhanced shear effects are exerted on the circular ribbon. Hereafter, we analyse the interaction with the tube wall by (4.1). It implies that the diffusion along the streamwise direction is enhanced, and the solution will disperse from its two ends along the tube wall in both the positive and negative directions of x. At the front end of the ribbon, $\partial C/\partial x < 0$. Therefore, we have the cross-effect $-2\,Pe\,tr\,\partial C/\partial x > 0$. With the aid of the zero-flux condition in the radial direction, we deduce that $\partial C/\partial r > 0$ at $r = 1$. Physically, the shear effect tends to make the solution disperse in the positive radial direction towards the wall. Likewise, for the rear end of the ribbon, the cross-effect makes the solution disperse towards lower r.

We then focus on convection due to horizontal gradients and lateral diffusion. On the inner surface of the ribbon, $\partial C/\partial r > 0$. With the aid of the zero-flux condition in the radial direction, we deduce that $2\,Pe\,tr\,\partial C/\partial x < 0$ and thus $\partial C/\partial x < 0$. Physically, the enhanced effect tends to make the solution disperse towards the negative direction of x. Convection occurs because horizontal variations in concentration are produced by the radial diffusion. Similarly, for the outer surface contacting the wall, we can indicate that the enhanced effect tends to disperse the solution towards positive x.

The foregoing analysis gives a picture of how the ribbon is distorted in a tube flow. To illustrate the shear effect and interaction with the wall boundary, we further explore how the asymmetries are caused by diffusion and interaction with the tube wall. As shown in figure 4, the initial concentration distribution of the ribbon is uniform. Due to the shear enhancement, the ribbon's shape would be distorted. Relative to the front part, the rear of the ribbon tends to spread radially more towards the tube axis, and then the inner solution tends to disperse axially more towards the negative direction. Caused by the interaction with the wall, the solute retaining near the wall disperses inwards and backwards. Hence the rectangular shape of mean concentration by the pure convection evolves gradually into a skewed platform, with an asymmetric peak in the rear part, as shown in figure 4. The manifestation of this asymmetry has emerged frequently in the development of both area and point sources. For instance, the initial area source and convection-induced rectangles both experience this kind of symmetry breaking. For the case of a uniform discharge, Chatwin (1970) interpreted the evolution with his physical intuition. The interpretation could be extended on a rigorous basis of mathematical formulae for wider initial sources. The strength of our derivation (3.29) lies in its compactness and simplicity with the combination of precision in quantity. As illustrated in figure 3, it also outweighs as an analytical particular solution from the very initial release towards the transitional stage.

4.2. *Persistence of asymmetries and their origins*

With the understanding that a direct Gaussian approximation could not reproduce the multi-peaked structure (Smith 1982*b*), efforts directly from the solution of Saffman or Taylor should contribute little in effect to feature the 'skewed platform' in figure 4. Since the asymmetries could be persistent, it is of research interest to investigate the following questions. (i) What are the origins of the symmetry breaking of mean concentration

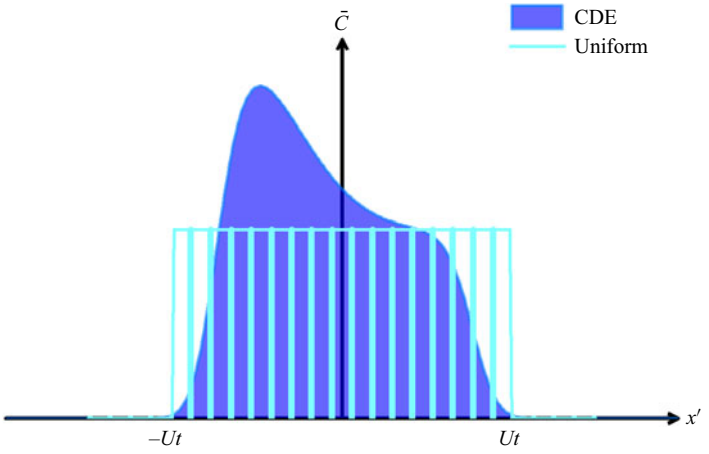

Figure 4. Physical interpretation of the uniform distribution to the asymmetric platform caused by the shear effect and interaction with the wall. The filled graph is computed by full numerical solutions of the convection–diffusion equation (CDE), and the cyan line is predicted by the pure advection model as a uniform distribution from an area source at $t = 0.15$.

distribution? (ii) What physical patterns could emerge during the convection–diffusion process, as time elapses from 0 to ∞?

First, the initial distribution could be inhomogeneous in its own right. This initial non-uniformity of the soluble matter could be rather persistent before reaching the Taylor dispersion regime. In terms of moments and cumulants, the skewness may deviate from zero initially, thus mean concentration could be asymmetric. Hence an origin of asymmetries along the axial direction is present soon whether or not the ribbon is distributed uniformly initially.

Second, the unidirectional convective distortion plays an important role in symmetry breaking. For instance, the cloud of soluble matter could have a long-tailed distribution as shown in figure 5, stretched either upstream or downstream. This remarkable feature is first captured qualitatively by a pure advection model of Taylor (1953) from a point moving at the mean speed of the flow.

Third, the zero-flux effect of the wall boundary serves as another origin of asymmetries. The zero-gradient boundary condition at the wall ($\partial C/\partial r = 0$), in the convected coordinate becomes a zero diffusion flux condition ($\partial C/\partial r + 2\,Pe\,tr\,\partial C/\partial x = 0$) at $r = 1$. The interaction with the wall gives rise to typically skewed platforms, which are highly unsymmetrical. We confirm in figure 5 that the asymmetry can be caused by only diffusion and interaction with the wall.

In summary, we certify theoretically that the asymmetries of concentration distribution through a circular tube have at least three origins, basically: (a) initial non-uniformity, (b) unidirectional convective distortion, and (c) zero-flux effect of wall boundary.

In figures 4 and 5, the pure advection solution and short-time diffusion solution are illustrated to show the origins of the asymmetric physical patterns, which still deviate from the convection–diffusion equation for specific times during the transitional stage. The mismatch is obviously due to the cross-effect, i.e. the second term on the right-hand side of (3.22), and low-order image approximations of the boundary effect, which precludes the soluble matter from being rotated and elongated into a more skewed and smooth profile.

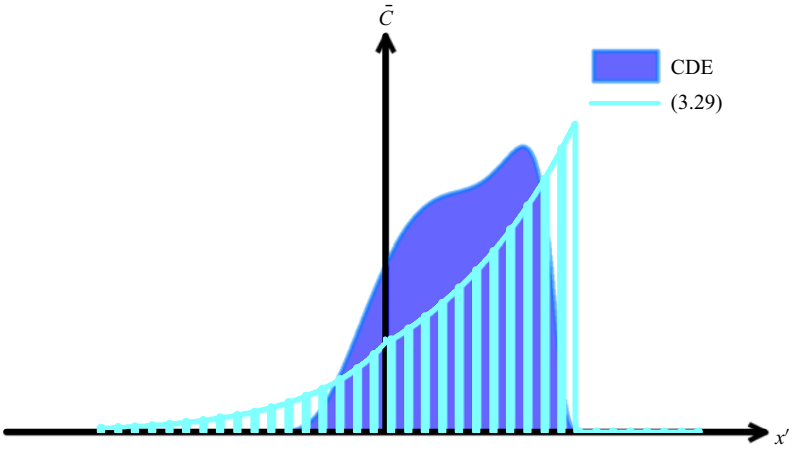

Figure 5. Physical interpretation of the long-tailed distribution to the asymmetric platform caused by the shear effect and interaction with the wall. The filled graph is computed by full numerical solutions of the convection–diffusion equation (CDE), and the cyan line is predicted by (3.29) from a central point source at $t = 0.2$.

Likewise, the enhanced diffusion effect, i.e. the third term on the right-hand side of (3.22), would shape the rectangular profile into a symmetric Gaussian form.

Before approaching the second problem, we would like to exemplify the transient dispersion from a point source to illustrate the symmetry breaking during the temporal evolution of concentration distributions. The fundamental case gives a comprehensive picture of how the diffusion process translates from one pattern to another as time elapses. For the transient dispersion of a solute discharged from a point source on the axis, there are virtually four dispersion regimes developing incrementally, say a longitudinal diffusive regime, two transitional (anomalous diffusion and pre-asymptotic) regimes, and a Taylor dispersion regime from an initially short time to asymptotically long times. With the Monte Carlo simulation, we illustrate the four dispersion regimes with corresponding transverse and mean concentration distributions as presented in figure 6. For short times, the longitudinal diffusion is predominant over either convection or radial diffusion. Provided that a blob of point sources is injected into the lateral position far from the wall, the solute cloud will diffuse isotropically, in the convected coordinate system. In other words, the spread of the point source follows a modified Gaussian distribution initially as shown in figure 6(*c*). The anomalous diffusion regime is an intermediate stage where complicated balance mechanisms occur. The widely recognised pure convection model is applicable to this stage, as is Lighthill's exact solution (Lighthill 1966). However, it should be noted that Lighthill's solution imposed impractical limitations, potentially rendering the predictions inconsistent with the physical manifestation of the natural dispersion process. In fact, the mean concentration distribution should exhibit a rectangular shape as predicted neither by the pure advection model due to the neglect of lateral diffusion, nor by Lighthill's modified approximation due to the neglect of wall effect. Lighthill's exact solution serves as an interaction mechanism within the anomalous diffusion regime, distinct from the initial stage. Subsequently, this facilitates the examination of lateral diffusion influenced by boundary walls and convection. Consequently, there exist two balance mechanisms before and after the unachievable pure advection stage. The former is influenced predominantly by longitudinal diffusion and advection, while the latter is affected primarily by advection and lateral diffusion. The interaction between tube walls

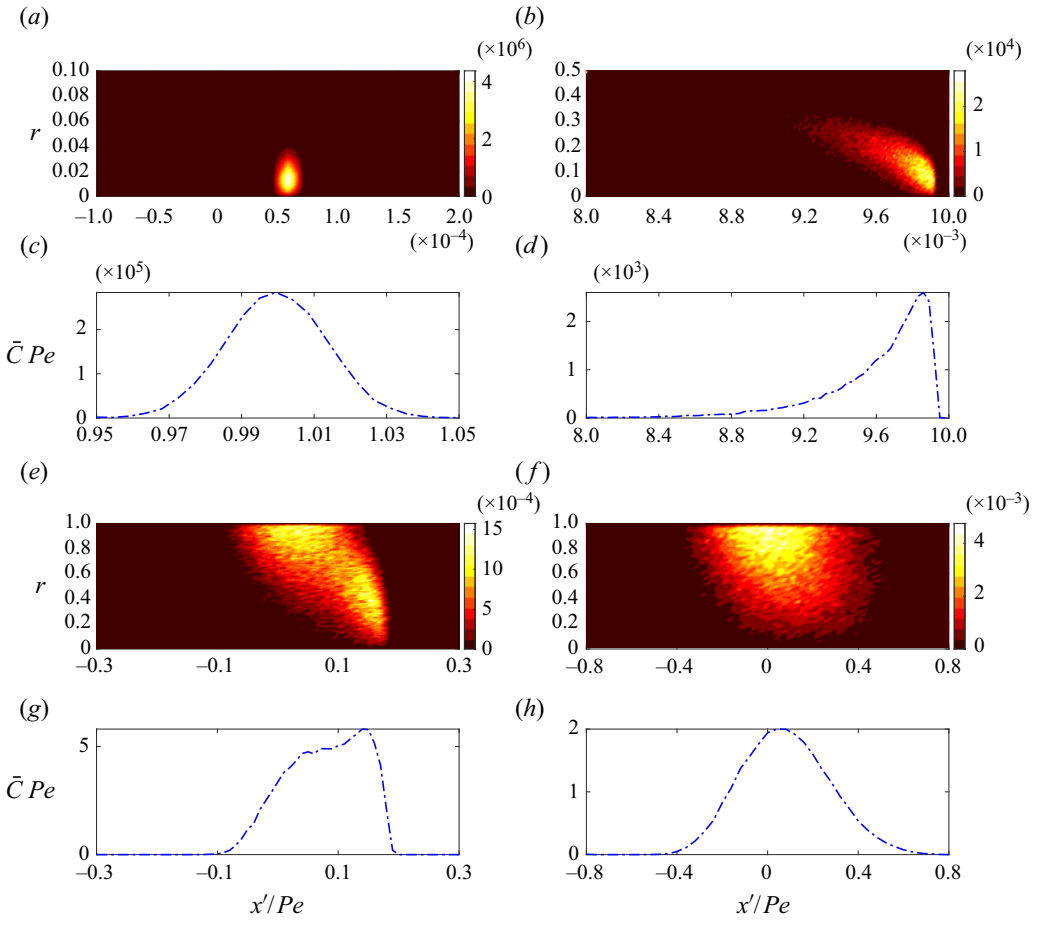

Figure 6. Four dispersion regimes in the transient dispersion (after figure 2 on p. 402 of Latini & Bernoff 2001). The azimuthally averaged concentration distributions of a solute in the tube with rotational symmetry are calculated with the Monte Carlo simulation, with the two-dimensional concentration contours and mean concentration $\bar{C}$ line graphs plotted as functions of the longitudinal axis x and/or radial axis r. (*a*,*c*) The longitudinal diffusive regime at $t = 1.0 \times 10^{-4}$. (*b*,*d*) The anomalous diffusion regime at $t = 1.0 \times 10^{-2}$. (*e*,*g*) The pre-asymptotic regime at $t = 2.0 \times 10^{-1}$. (*f*,*h*) The Taylor dispersion regime at $t = 1.0$. Common parameters are $Pe = 10\,000$ and $r_0 = 0$.

and particles in the presence of external hydrodynamic conditions leads to the emergence of symmetry breaking and multi-scale characteristics, which align with the transition between these two mechanisms. Technically, it remains most difficult to account for this transition from the anomalous diffusion stage to the pre-asymptotic regime, shown in figures 6(*d*,*g*). For asymptotically long times, Taylor (1953) described the enhanced longitudinal dispersion under the combined action of advection and lateral diffusion. In particular, the longitudinal normality ($t \gtrsim 1$; Chatwin 1970) and transverse uniformity ($t \gtrsim 10$; Wu & Chen 2014) have been explored systematically, as shown in figure 6(*h*).

5. Streamwise dispersion model

In this section, a streamwise dispersion model is formulated by matching the limiting particular solutions, and examined in the classical Poiseuille tube flow. Typical initial

distributions including the area and point sources are discussed and verified. To review and extend the classical results of Aris (1956) and Chatwin (1970) and others, the instantaneous releases of main interest here are typical cases of area, point and ring sources. The influence of releasing positions of ring sources is investigated in terms of streamwise dispersivity and mean concentration. Transverse and mean concentration distributions are of crucial interest for the dispersion process. To verify quantitatively the streamwise dispersion model, we simulate numerically the advective–diffusion equation, and corroborate the analytical solutions with numerical results. Extensions of the model to a channel flow are discussed briefly in § 2 of the supplementary material.

5.1. *Streamwise dispersion model in local moment space*

To further investigate the second question posed in § 4.2, we revisit the convectively transformed governing equation (3.22). The equivalent transformed equation indicates a superposition of three effective diffusion processes. The second concern then transforms into how the effective diffusion processes take turns to dominate. From (3.28), which applies to short times after a discharge from the initial point source, the concentration distribution asymptotes to a modified Gaussian form. For longer times, the cross-shear effect – i.e. the second term on the right-hand side of the convectively transformed governing equation – is predominant to introduce asymmetries. When the solute cloud approaches the wall, the interaction with the wall will further lead to symmetry breaking. For asymptotically long times, the enhanced streamwise diffusion term along the axial direction – i.e. the third term on the right-hand side of the convectively transformed governing equation – dominates other contributions. This paves the way naturally to the Taylor dispersion model, i.e. the convection–diffusion process is characteristic of one-dimensional enhanced diffusion for asymptotically long times. Taylor (1953) made an assumption that the effective diffusivity is independent of time or space. Based on a Taylor expansion of concentration distribution at the vicinity of mean concentration, the dispersivity can be derived by inversion. Note that the formal convection–diffusion process belongs intrinsically to diffusion type from the perspective of the moving fluid particles, whilst the effective diffusivity should vary nonlinearly with time and anisotropically in space.

The limitation of (3.22) for analytical approaches is that nonlinear terms make it hard to be mathematically tractable. However, we emphasise that the general convection transformation and short-time particular solution reveal novel physical structures of transient dispersion. From the implications of the convectively transformed equation, an exact diffusion-type description is formulated. We can make use of the exact solutions of local concentration moments to determine the nonlinear diffusion coefficients. We will formulate a streamwise expansion matching the convection transformation in local moment space, with the aim of reproducing accurately the featured physical structures.

Upon utilising a convection transformation, the short-time particular solution of concentration of pointwise soluble matter follows a modified Gaussian distribution viewing from the fluid particles. The short-time particular solution of the convection–diffusion equation is derived from the perspective of fluid particles valid for times before most soluble matter approaches the boundary wall, complementary to the Taylor dispersion model. It is predicted and verified that a tilted Gaussian distribution of concentration appears long before a paraboloidal snout has been pulled out by the Poiseuille tube flow, which later skews when colliding with the wall, and eventually disperses into an equilibrium Taylor dispersion state. On the other hand, the long-time

convectively transformed equation also implies an asymptotic dispersion solution of point discharge in a bounded flow, corresponding to a typical Gaussian distribution as suggested originally by Taylor (1953).

The basic mechanism of Taylor dispersion is general in both cases, even though Gaussian approximation may fail in the transition stage. A significant advance of Smith (1982*b*) for a Gaussian approximation along the streamline with a uniform area source stems from the short-time approximated source solution of Saffman (1960) and the long-time Gaussian solution of the Taylor dispersion model. He was disappointed that a direct Gaussian approximation could not reproduce the asymmetric characteristics and later designed a delay–diffusion model (Smith 1981, 1982*a*). Aimed at the inaccuracy of the Gaussian approximation of Smith (1982*b*) for asymptotically short times, Li (2018) extended the Taylor–Aris method for the transverse concentration in the spirit of streamwise dispersion. This second-order Taylor–Aris description could not only depict well the early stage whence the transport of the solute is governed by longitudinal diffusion and convection, but also recover the long-time evolution of dispersion without resorting to higher-order terms. The basic asymmetric physical structure is produced qualitatively for the first time as a breakthrough. However, the quantitatively satisfactory reproduction of asymmetric physical structures, especially during the pre-asymptotic regime, still remains desirable yet elusive to date. A streamwise expansion from the asymptotic analysis shows that the concentration distribution is subject to a modified Gaussian distribution in local moment space. By taking into account the Edgeworth modification in statistical theory, a streamwise dispersion model would be devised to fill in this gap.

A streamwise coordinate, which moves initially at the local velocity of the external flow field and eventually at the mean flow speed, naturally comes from these two limits, as will be normalised later, in (5.6). Define the marginal probability density function P as

$$P(\xi, r, t \,|\, \xi_0, r_0) = \frac{C(\xi, r, t)}{\displaystyle\int_{-\infty}^{\infty} C(\xi, r, t)\,\mathrm{d}\xi}, \tag{5.1}$$

which gives the probability of the tracer present at the point (ξ, r) at time t, given its initial release at the point (ξ_0, r_0). The Fourier transform of the probability density function gives the cumulant-generating function with respect to the angular frequency k as

$$\phi(k, r, t) \equiv \int_{-\infty}^{\infty} P \exp(\mathrm{i}k\xi)\,\mathrm{d}\xi. \tag{5.2}$$

This cumulant-generating function could be obtained with the natural logarithm (Kendall & Stuart 1958; Chatwin 1970; Jiang & Chen 2018) as

$$\ln\phi = \sum_{n=1}^{\infty} \kappa_n \frac{(\mathrm{i}k)^n}{n!}, \tag{5.3}$$

wherein κ_n is the nth-order cumulant, which could be obtained directly through central moments, as is computed in the supplementary material. Substitution of (5.3) into the inverse transform of ϕ gives

$$\frac{C(\xi, r, t)}{\displaystyle\int_{-\infty}^{\infty} C(\xi, r, t)\,\mathrm{d}\xi} = \frac{1}{2\pi}\int_{-\infty}^{\infty} \exp\left[\sum_{n=1}^{\infty} \kappa_n \frac{(\mathrm{i}k)^n}{n!}\right] \exp(-\mathrm{i}k\xi)\,\mathrm{d}k. \tag{5.4}$$

Note that the denominator on the left-hand side is the zeroth moment. That is, the streamwise expansion inherently gives the relationship between concentration distribution and moments. Using the identity

$$\int_{-\infty}^{\infty} \exp\left(-\mathrm{i}k\xi - \frac{1}{2}k^2\right)(\mathrm{i}k)^n \,\mathrm{d}k = \sqrt{2\pi}\, He_n(\xi) \exp\left(-\frac{1}{2}\xi^2\right), \tag{5.5}$$

the Taylor expansion of the first exponential term on the right-hand side of (5.4), and Edgeworth's modification (Kendall & Stuart 1958; Chatwin 1970) embodied by square brackets, we could obtain a concise and accurate streamwise expansion with the normalised Eulerian coordinate as

$$\begin{aligned} C(\xi, r, t) = \frac{C_0}{\sqrt{2\pi\kappa_2}} \exp\left[-\frac{(\xi-\kappa_1)^2}{\kappa_2}\right] \times \left\{1 + \left[\frac{\kappa_3}{3!(\kappa_2)^{3/2}} He_3\left(\frac{\xi-\kappa_1}{\kappa_2^{1/2}}\right)\right]\right. \\ \left. + \left[\frac{\kappa_4}{4!\,\kappa_2^2} He_4\left(\frac{\xi-\kappa_1}{\kappa_2^{1/2}}\right) + \frac{10\kappa_3}{6!\,\kappa_2^3} He_6\left(\frac{\xi-\kappa_1}{\kappa_2^{1/2}}\right)\right] + \cdots\right\}, \end{aligned} \tag{5.6}$$

where $C_n(r,t) \equiv \int_{-\infty}^{\infty} C(\xi, r, t)\,\xi^n \,\mathrm{d}\xi \;\; (n = 0, 1, 2, \ldots)$ is the nth-order moment of concentration, and He_n is the Chebyshev–Hermite polynomial of nth order. Physically, κ_1 represents the advection velocity along each streamline, κ_2 is the streamwise mean square displacement applied to ensure unit variance for long times, κ_3 is the streamwise skewness quantifying the extent of asymmetry, and κ_4 is the streamwise kurtosis reflecting the sharpness of the peak. Note that this choice of streamwise coordinate well matches the spirit of streamwise theory in local moment space. While the basic term beyond the expansion is a unified expression for both the short- and long-time Gaussian distributions, the expansion in the bracket includes the Edgeworth modification. This well-known Edgeworth form of the Gram–Charlie series of type A in statistical theory is introduced in (5.6) to collect terms of the same order as manipulated in each square bracket and improve the convergence of the analytical model, as a reflection of transient effects.

Especially for the high-order terms, usual truncation methods would ignore corresponding contributions in the same order of magnitude with the assumption $\kappa_n = O(t^{1-n/2})$. Comparison of the present streamwise expansion with the original models of Chatwin (1970), Gill *et al.* (1970) and Smith (1982*b*) will be made intensively in § 5.3 and § 5.4. The present streamwise expansion outweighs others for the current application of fundamental Dirac delta sources due to its accurate description of moments and superior astringency, whereas the generality of the streamwise dispersion theory is not affected. Significant improvement would be shown especially during the transitional regime before Taylor dispersion, in contrast to existing analytical models.

Streamwise dispersion of soluble matter subject to longitudinal advection and transverse diffusion is often described by an averaged dispersion coefficient over the cross-section. By extending further the Taylor dispersion theory, new definitions of this averaged amount for the effective diffusion coefficients in (5.11) should be adopted, however, to better capture the streamwise characteristics. In contrast to the coarse-grained Taylor–Aris dispersivity $\bar{D}_T$ defined as

$$\bar{D}_T = \frac{1}{2}\frac{\partial}{\partial t}[\bar{C}_2 - (\bar{C}_1)^2], \tag{5.7}$$

Yasuda (1984) proposed a new averaging method

$$\bar{D}_T^S = \frac{1}{2}\frac{\partial}{\partial t}\left[\overline{\frac{C_2}{C_0} - \frac{C_1^2}{C_0^2}}\right], \tag{5.8}$$

where the overbar denotes a transverse averaging operator over the cross-section, to avoid the presence of negative streamwise dispersivity. The latter is denoted with a superscript S to show its accuracy of streamwise information. Note that the asymptotic values yield to Taylor dispersivity $1 + Pe^2/48$ through a straight circular tube. Hereafter, we resort to these two definitions of transverse averaging of time-dependent effective diffusion coefficients, normalised by the asymptotic Taylor dispersivity, for better understanding of non-trivial and heuristic results of streamwise dispersion. The spatio-temporal evolution of time-dependent effective diffusion coefficients, commonly termed as transient dispersivity, is shown in figure 7, wherein the power of streamwise theory is revealed clearly. For long times, it is shown that the dispersion grows linearly with time, and dispersivity approaches transverse uniformity, whence the solute molecule has taken identical opportunity to sample the whole tube cross-section. This dispersion occurs due to the stochastic nature of radial Brownian diffusion; not all soluble matter discharged initially at $\xi = 0$ will leave a fixed exit plane in the meantime. In other words, a distribution of transient dispersivity exists before the dispersion regime as displayed in figure 7(*a*).

Different initial conditions are adopted in figure 7(*b*), and the transient streamwise dispersivity about the mean uncovers a peculiar characteristic peak that perceptibly exceeds the Taylor–Aris limit ($1 + Pe^2/48$), which was reported through straight channels of arbitrary cross-section by Vedel *et al.* (2014) for the first time. This interesting phenomenon is due to the delay of relaxation time between the first and second axial moments (Vedel *et al.* 2014). Only releases near the central axis could produce the unique peak in contrast to dispersion from uniform area and near-wall point sources or purely dissipative process like diffusion. Note that this non-monotonic variation of transient streamwise dispersivity corresponds to some particular dispersion regimes, from a fundamental level of probability density distribution. For example, the motion from a central point source is diffusive for the initial regime, then varies from super-diffusive to sub-diffusive during the anomalous regime, and eventually becomes diffusive once again within the dispersion regime. This peculiar characteristic peak of transient streamwise dispersivity could not only be mathematically understood from the deviation of first and second moments, but also physically explained as being a point from the classical continuum-mechanical perspective. The statistical trajectory of this locator point could represent the spreading of a solute through the flow. Released near the axis of the tube, the solute diffuses transversely from the centre to the wall before its approach to uniformity. The intrinsic convection of Poiseuille tube flow drives particles on the axis faster than those near the wall, leading to an enhanced axial spreading of the tracer in the presence of molecular diffusion compared to the fluid particle. This is responsible for the monotonic increase of streamwise dispersivity during the initial regime. Later, the effect of boundary sets in when the locator point diffuses radially outwards towards the wall, which results transiently in an asymmetric platform of concentration distribution and characteristic peak of streamwise dispersivity. The highly remarkable nonlinear contribution of Taylor dispersion with respect to molecular diffusivity from axial diffusion arises exactly from transverse molecular diffusion and axial convection. The smaller the molecular diffusivity, the more appreciable enhanced dispersion occurs. Before the locator solute behaves identically with the fluid particle in a kinematic sense in the long run, the transverse

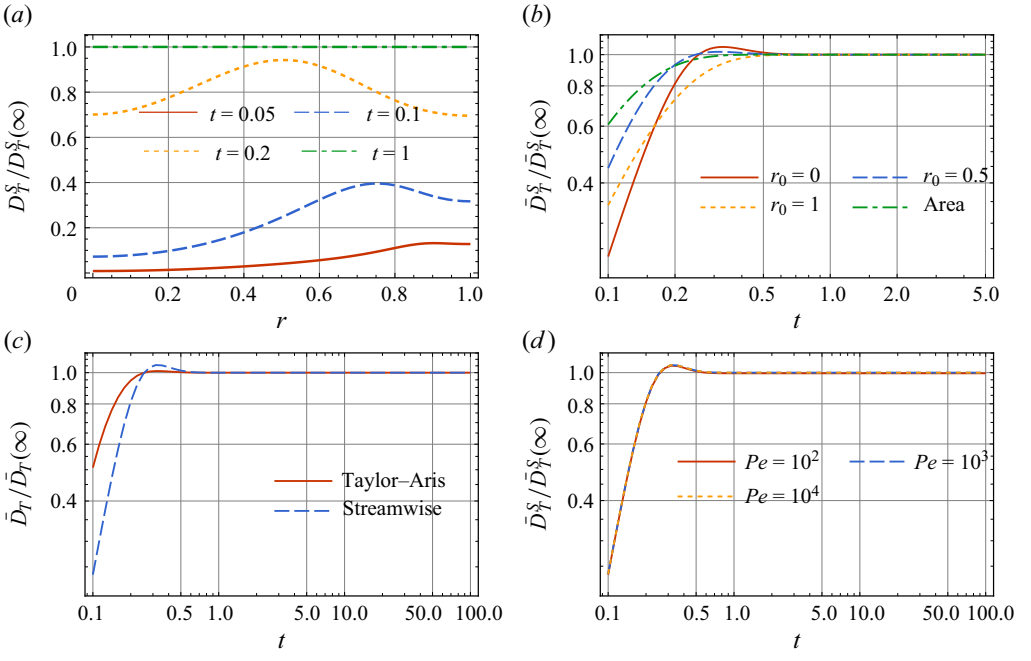

Figure 7. Spatio-temporal evolution of time-dependent effective diffusion coefficients, normalised by the asymptotic Taylor–Aris limit ($\bar{D}_T(\infty) = 1 + Pe^2/48$). (*a*) Transient streamwise dispersivity of (5.11) in a tube Poiseuille flow for $Pe = 10\,000$ with a central point source as a function of r within different regimes. (*b*) Plot of the normalised streamwise dispersivity with $r_0 = 0, 0.5, 1$ and uniform area source. Peculiar characteristic peaks of transient dispersivity are revealed to exceed $\bar{D}_T(\infty)$ perceptibly. (*c*) Comparison of the coarse-grained Taylor–Aris dispersivity (5.7) and streamwise dispersivity (5.8) with $Pe = 10\,000$ and $r_0 = 0$. (*d*) The normalised streamwise dispersivity completely overlaps for different Péclet numbers, when streamwise variations in concentration due to advection remarkably outweigh molecular diffusion ($Pe \gg 1$).

positions across the tube indeed do not attract the solute molecule equally. This preferential behaviour of the asymmetric transverse distribution is the key to the biases of drift velocities and streamwise dispersivities. Within the pre-asymptotic dispersion regime, the effect of flow convection and reflective wall indeed attenuate the transverse diffusion, and thus result in an enhanced axial spreading even exceeding the Taylor–Aris limit.

Comparison of the coarse-grained Taylor–Aris dispersivity and streamwise dispersivity is shown in figure 7(*c*). Although the peculiar peaks are shown for both definitions from a central point release, we emphasise that only the streamwise dispersivity exactly captures the axial displacement along each streamline, and clearly exhibits the remarkable enhancement of axial spreading. The overall Taylor–Aris dispersivity is instead a fictitious quantity of the whole cloud of soluble matter, which may exhibit negative values at small times; see e.g. Yasuda (1984, figures 8 and 10, p. 395), Guan *et al.* (2021, figure 13, p. 12) and Guan *et al.* (2022, figures 11 and 12, pp. 14–15). As the crucial dimensionless parameter in this simple physical problem, the flow Péclet number quantifies the ratio of flow convection to molecular diffusion. In figure 7(*d*), we demonstrate that the normalised streamwise dispersivity completely overlaps with different Péclet numbers, when streamwise variations in concentration due to advection remarkably outweigh molecular diffusion. This limit is a requirement of Taylor dispersion, while its opposite limit could also be an interesting inverse problem outside the scope of this work. Although

Péclet number influences significantly the absolute values of streamwise dispersivity, the normalised quantities presented in this paper are unified to illustrate the exact evolution.

It would be captivating to establish a link between these observations and the physical manifestations of transient dispersion, as depicted in figure 6, revealing four distinct dispersion stages within this problem. At the outset, dispersion results primarily from streamwise diffusion, prevailing over shear effects, as depicted in figure 6(*a*). For a central point source, the concentration distribution takes the form of a modified Gaussian, being convected by the streamwise flow velocity, as depicted in figure 6(*c*). During this stage, the streamwise dispersivity exhibits a zero slope, resembling ordinary isotropic diffusion, and is represented as a diffusive regime by Latini & Bernoff (2001).

The interplay of shear-induced convection with molecular diffusion gives rise to anomalous scaling, causing non-monotonic variations in streamwise dispersivity. Within this stage, in this work we have delineated two distinct regimes, depending on whether streamwise or lateral diffusion takes precedence. As shown in figures 6(*d*,*g*), the hallmarks of the above regimes are tilted Gaussian distributions and one skewed platform-like distribution, respectively. The transition initiates once the majority of soluble substances have traversed the streamlines to interact with the boundary. It is important to note that a distinctive peak, exceeding the Taylor–Aris limit, becomes evident as the non-penetration boundary effect comes into play during tracer dispersion. This corresponds to the right-skewed distribution of mean concentration, indicating a significantly enhanced solute dispersion in the pre-asymptotic transitional regime. The developed streamwise dispersion model has the capacity to capture these novel statistical and physical characteristics of mean concentration, including the distinctive heads and tails of the asymmetric concentration profiles.

Over time, in the Taylor dispersion regime, particles gradually approach transverse uniformity and streamwise normality, as illustrated in figures 6(*f*,*h*). The streamwise dispersivity once again demonstrates diffusive scaling, albeit in a notably enhanced fashion. Moreover, the concentration distribution reverts to a streamwise Gaussian distribution, corresponding to the longitudinal Gaussian distribution in Taylor's model.

5.2. *Asymptotic analysis*

The asymptotic behaviours of the concentration moment have been explored extensively. Following Aris (1956) and Li (2018), we hereafter resort to the asymptotic analysis of the second-order streamwise model of transient dispersion, for both asymptotically short and long times. In this paper, the original coarse-grained Taylor–Aris drift velocity and dispersivity are denoted as $\bar{\Phi}_T(t)$ and $\bar{D}_T(t)$, respectively. Viewing in a rather distinct perspective, we can transform the velocity and diffusion coefficients in Taylor's model to the drift velocity and dispersivity in their full-time dependence, and a second-order governing equation of streamwise expansion is obtained equivalently (Li 2018) as

$$\frac{\partial C(\xi, r, t)}{\partial t} + \Phi_T^S \frac{\partial C(\xi, r, t)}{\partial \xi} = D_T^S \frac{\partial^2 C(\xi, r, t)}{\partial \xi^2}, \tag{5.9}$$

where the streamwise drift velocity is defined as

$$\Phi_T^S \equiv \frac{\partial \mu_1}{\partial t}, \tag{5.10}$$

and time-dependent streamwise effective diffusion coefficients are defined as

$$D_T^S \equiv \frac{1}{2} \frac{\partial \mu_2}{\partial t}. \tag{5.11}$$

The central moment μ_n up to second order reads

$$\mu_1(\xi, r, t) = \frac{C_1}{C_0}, \quad \mu_2(\xi, r, t) = \frac{C_2}{C_0} - \frac{C_1^2}{C_0^2}. \tag{5.12a,b}$$

The analytical solution of second-order streamwise dispersion theory could be derived as

$$C(\xi, r, t) = \frac{C_0}{\sqrt{2\pi(C_2/C_0 - 2C_1^2/C_0^2)}} \exp\left[-\frac{(\xi - C_1/C_0)^2}{2(C_2/C_0 - 2C_1^2/C_0^2)}\right]. \tag{5.13}$$

For transient dispersion through a tube from a uniform area source, the first moment of a discharge for long times reads

$$C_1(r, t) = Pe \sum_{j=1}^{\infty} \frac{J_0(\theta_j r)}{J_0(\theta_j)} \frac{\overline{J_0(\theta_j r)\, u}}{J_0(\theta_j)} \frac{1 - \exp(-t\theta_j^2)}{\theta_j^2}, \tag{5.14}$$

and the second moment is

$$C_2(r, t) = \bar{C}_2 + 2t + 2\,Pe^2 \sum_{j=1}^{\infty} \frac{\varphi_j^2}{\theta_j^2}\left[t - \frac{1 - \exp(-t\theta_j^2)}{\theta_j^2}\right] + \sum_{k=1}^{\infty} \frac{J_0(\theta_k r)}{J_0(\theta_k)} F_k(t), \tag{5.15}$$

where J_n denotes the Bessel function of the first kind of nth order, and θ_i denotes the eigenvalues as the positive roots of the transcendental equation $\theta_n J_1(\theta_n) = 0$. For asymptotically long times, we have

$$\lim_{t\to\infty} \frac{1}{2} \frac{\partial(C_2 - C_1^2)}{\partial t} = 1 + \lim_{t\to\infty} Pe^2 \sum_{j=1}^{\infty} \frac{\varphi_j^2}{\theta_j^2}[1 - \exp(-t\theta_j^2)] + \lim_{t\to\infty} \sum_{k=1}^{\infty} \frac{J_0(\theta_k r)}{J_0(\theta_k)} \frac{\partial F_k}{\partial t}, \tag{5.16}$$

wherein the differentiation of F_k with respect to t is defined as

$$\frac{\partial F_k}{\partial t} = Pe^2 \sum_{j=1, j\neq k}^{\infty} \varphi_j \varphi_{jk} \frac{\exp(-t\theta_k^2) - \exp(-t\theta_j^2)}{\theta_j^2 - \theta_k^2} + \frac{1}{3} Pe^2\, \varphi_k t \exp(-t\theta_k^2), \tag{5.17}$$

and the coefficients φ_j and φ_{jk} are obtained as

$$\varphi_j = \int_0^1 2u \frac{J_0(\theta_j r)}{J_0(\theta_j)} r\, \mathrm{d}r, \tag{5.18}$$

$$\varphi_{jk} = \int_0^1 2u \frac{J_0(\theta_j r)}{J_0(\theta_j)} \frac{J_0(\theta_k r)}{J_0(\theta_k)} r\, \mathrm{d}r, \quad j \neq k. \tag{5.19}$$

With simple substitution, the streamwise drift velocity at asymptotically long time is derived as

$$\lim_{t\to\infty} \Phi_T^S = \lim_{t\to\infty} \frac{\partial C_1}{\partial t} = \lim_{t\to\infty} Pe \sum_{j=1}^{\infty} \frac{J_0(\theta_j r)}{J_0(\theta_j)} \frac{\overline{J_0(\theta_j r)\, u}}{J_0(\theta_j)} \exp(-t\theta_j^2) = 0, \tag{5.20}$$

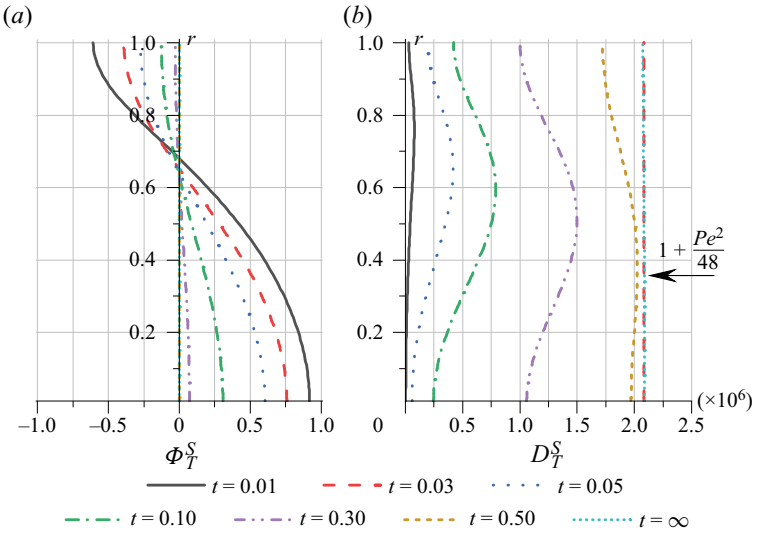

Figure 8. Plots of (*a*) Φ_T^S and (*b*) D_T^S as functions of r at different times, for $Pe = 10\,000$ from an area source.

and the corresponding asymptotic streamwise dispersivity is

$$\lim_{t\to\infty} D_T^S = \lim_{t\to\infty} \frac{1}{2}\frac{\partial(C_2 - C_1^2)}{\partial t} = 1 + Pe^2 \sum_{j=1}^{\infty} \frac{\varphi_j^2}{\theta_j^2} = 1 + \frac{Pe^2}{48}. \tag{5.21}$$

Note that D_T^S and Φ_T^S yield to be constant at long times, and equal to coefficients of the original Taylor–Aris model, as shown in figure 8. That is, the second-order streamwise model is equivalent to Taylor's dispersion model valid for asymptotically long times, whereas the equivalent diffusivity is a nonlinear function of time and space coordinates.

On the other hand, the following results will show that the streamwise dispersion model can also be appropriate for asymptotically short time. For a short time from an area source,

$$\lim_{t\to 0} \frac{1}{2}\frac{\partial(C_2 - C_1^2)}{\partial t} = 1 + \lim_{t\to 0} Pe^2 \sum_{j=1}^{\infty} \frac{\varphi_j^2}{\theta_j^2}\,(1 - \exp(-t\theta_j^2)) + \lim_{t\to 0} \sum_{k=1}^{\infty} \frac{J_0(\theta_k r)}{J_0(\theta_k)}\frac{\partial F_k}{\partial t}. \tag{5.22}$$

With simple substitution, the drift velocity of the second-order streamwise expansion for an asymptotically short time is derived as

$$\lim_{t\to 0} \Phi_T^S = \lim_{t\to 0} \frac{\partial C_1}{\partial t} = \lim_{t\to 0} Pe \sum_{j=1}^{\infty} \frac{J_0(\theta_j r)}{J_0(\theta_j)}\frac{\overline{J_0(\theta_j r)\,u}}{J_0(\theta_j)} \exp(-t\theta_j^2) = Pe\,u, \tag{5.23}$$

and the corresponding asymptotic effective diffusion coefficient is

$$\lim_{t\to 0} D_T^S = \lim_{t\to 0} \frac{1}{2}\frac{\partial(C_2 - C_1^2)}{\partial t} = 1. \tag{5.24}$$

Substituting the asymptotic Φ_T^S and D_T^S into the streamwise expansion gives

$$\frac{\partial C}{\partial t} + Pe\,u(r)\frac{\partial C}{\partial \xi} = \frac{\partial^2 C}{\partial \xi^2}. \tag{5.25}$$

Comparing (5.25) with (3.1), the difference lies in the diffusion terms over the cross-section. In other words, (3.1) can be reduced to (5.25) at asymptotically short times. It shows that the dispersion process during the initial stage is dominated by the combined action of longitudinal diffusion and advection. The lateral diffusion terms are smeared out mathematically for the second-order model from an area source, as the initial and eventual uniform distributions for asymptotically short and long times guarantees its accuracy. For point sources, the lateral diffusion could not be neglected, while its effect should be incorporated by higher-order cumulants, especially for the transitional stage. Due to the attractive mathematical properties of the Dirac delta function, we will pay special attention to the application of the higher-order streamwise dispersion model in terms of area and central point sources at a large Péclet number. Further elucidation on the effects of Péclet numbers and initial conditions can be found in § 3 of the supplementary material.

5.3. *Uniform area source*

As a widely used model, we begin with the initial condition of the transversely uniform area source

$$C(\xi, r)|_{t=0} = \delta(\xi), \tag{5.26}$$

which is a fundamental initial condition explored extensively by previous work. A hallmark of the transient evolution of mean concentration is the transition from the skewed 'platform' towards the symmetric Gaussian distribution, while transverse distribution exhibits non-uniform towards asymptotically uniform features (Chatwin 1970; Smith 1982*b*; Houseworth 1984). The comparison of the analytical solutions for the streamwise dispersion model with the numerical results will give a quantitative test from the very initial release towards the dispersion regime. During the initial stage of transient dispersion, mean concentration distribution skews to form a peaked platform. Lighthill (1966) predicted a rectangular shape downstream for the positive x-axis, but was incapable of describing the rear part. Chatwin (1970) further interpreted this platform qualitatively with his strong intuition – however, without quantifying this distribution. It has disappointed Smith (1982*b*) that his Gaussian approximation fails to reproduce the bimodal physical structure of the exact concentration profile, and he came to the conclusion that the critical time of the Gaussian approximation is limited about one e-folding time scale. In contrast, we show that a diffusion-type streamwise dispersion model would be able to capture the skewed platforms satisfactorily for $t \sim 0.01$, as shown in figure 9(*a*). It is important to note that Gibbs phenomena are observed at short times in the context of fourth-order streamwise expansions. This outcome is clearly attributed to the numerical dispersion inherent in higher-order expansions, which does not impact the model's efficiency or hinder the attainment of physical insights. Indeed, these concerns have been raised by previous studies, and they are amenable to technical resolution (Mercer & Roberts 1990, 1994; Taghizadeh *et al.* 2020). The dispersion models of Chatwin (1970) and Gill *et al.* (1970) almost overlapped with each other as biased Gaussian distributions, albeit incapable of reproducing the skewed platform. As shown in figure 9, the present model demonstrates nicely how the rectangular shape evolves into a skewed platform with an asymmetric peak in the rear. This asymmetric feature is well predicted by the streamwise expansion of transient dispersion, which is caused by the shear effect and interaction with the wall.

For long times, the concentration distribution asymptotes to normality as described by Taylor (1953). However, distinct asymmetries persist before the Taylor–Aris limit, as illustrated in figure 10. The developed streamwise dispersion model and its fourth-order

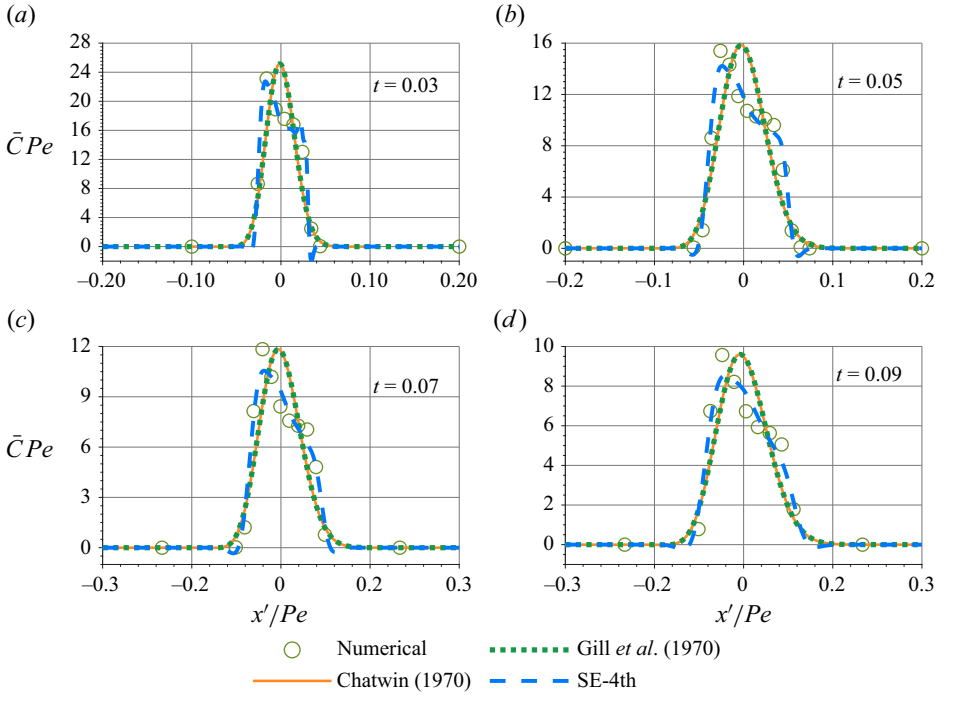

Figure 9. Axial distributions of mean concentration from an area source at short times obtained by Chatwin (1970), Gill *et al.* (1970) and the fourth-order streamwise expansion (marked as SE-4th) compared to the numerical results for $Pe = 10\,000$.

solution include the transient effect of streamwise skewness and kurtosis, thus effectively capturing the skewed and peaked distribution better than the existing Taylor models. It also reproduces the peak values as well as heads and tails more accurately, as a concise and compact description above all.

Contours of the two-dimensional concentration distribution of a solute for the area source discharge are obtained and illustrated in figure 11, compared with the full numerical solution of the convection–diffusion equation. The distinctive features are the non-uniform distribution across the streamlines. Physically, these can be explained by the basic origins of asymmetries, namely unidirectional convective distortion and the zero concentration flux at the walls in the current case of uniform area source. The streamwise expansion could well predict the concentration contours from the initial release to Taylor dispersion. Peculiar island-shaped structures of transverse concentration from a uniform area source are revealed in figures 11(*a*,*b*), during the pre-asymptotic regime. Obviously, for longer times the present streamwise expansion would behave as satisfactorily as the Taylor dispersion model that has been verified experimentally, as demonstrated by long-time asymptotic analysis in § 5.2.

5.4. *Central point source*

For an azimuthally asymmetric initial distribution released at $\xi = 0$ and $r = r_0$, we have specified

$$C(\xi, r)|_{t=0} = \delta(\xi)\,\frac{\delta(r - r_0)}{2r_0}. \tag{5.27}$$

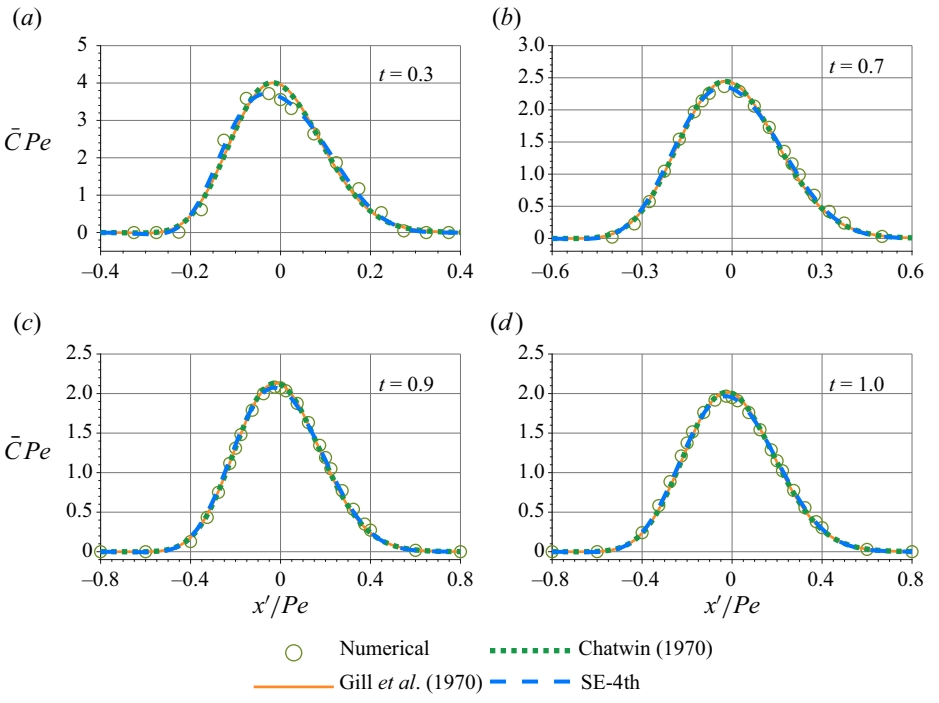

Figure 10. Axial distributions of mean concentration from an area source at long times obtained by Chatwin (1970), Gill *et al.* (1970) and the present (fourth-order) streamwise expansion compared to the numerical results for $Pe = 10\,000$.

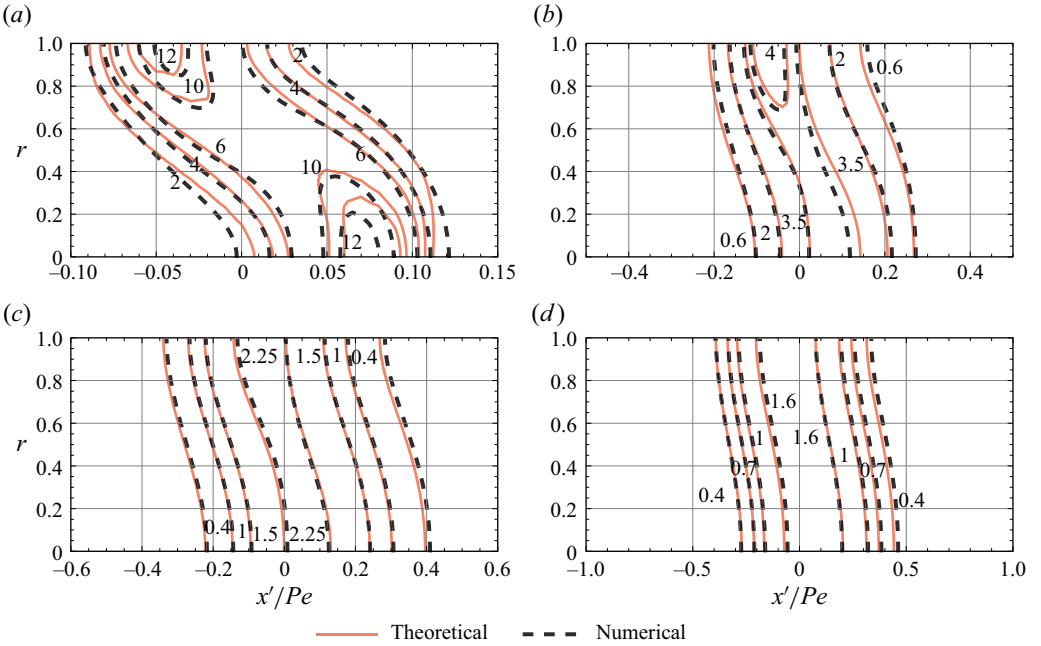

Figure 11. Contours of azimuthally averaged concentration distribution from an area source for $Pe = 10\,000$ obtained by the present (fourth-order) streamwise expansion compared to the numerical results.

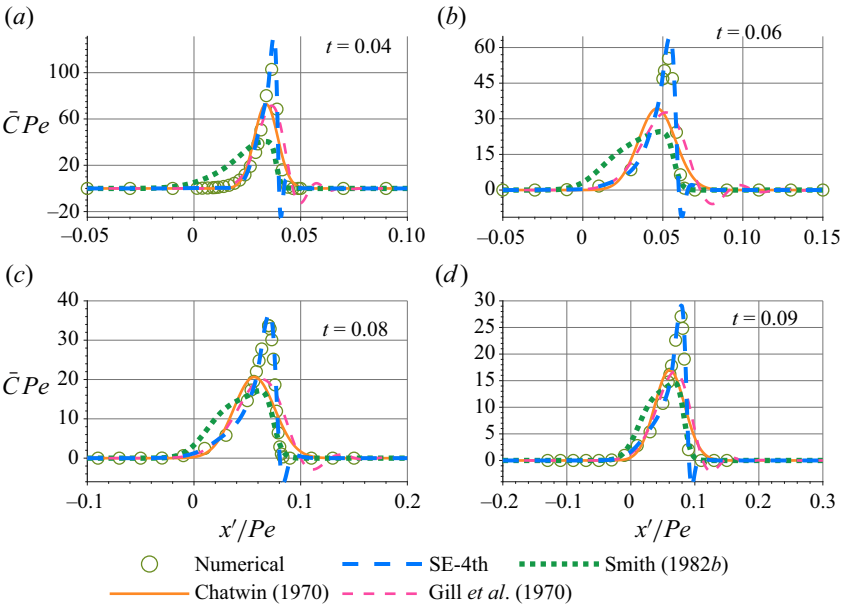

Figure 12. Axial distributions of mean concentration at short times obtained by Smith (1982*b*), Chatwin (1970), Gill *et al.* (1970) and the present (fourth-order) streamwise expansion compared to the numerical results. Common parameters are $Pe = 10\,000$ and $r_0 = 0$.

The ring source (Houseworth 1984; Debnath *et al.* 2022) could reduce to a special central point source when $r_0 \to 0$. This point source is another idealised physical model, with practical and fundamental research interest as models of droplets of drugs injected into human blood (Fallon, Howell & Chauhan 2009) and contaminant discharged into sewage treatment industries (Chatwin & Allen 1985). To illustrate the applicability of the streamwise dispersion model, point and ring sources released at different positions are examined in this work.

During the initial stage of transient dispersion for the central point source release, a long-tailed distribution of the cloud of the soluble matter is appreciable. This remarkable physical structure is due to the combined effect of unidirectional convective distortion and molecular diffusion. This structure is also predicted satisfactorily by the particular solution (3.28). Latini & Bernoff (2001) gave a compact derivation for the head and tail distributions, respectively. As shown in figure 12, the present streamwise expansion accounts accurately for this physical structure. Compared to the results of Chatwin (1970), the analytical approach to normality would not be sufficient to predict the short-time concentration distribution. The amplitude and phase of the mean concentration are predicted satisfactorily by an analytical solution of the present streamwise model, compared with numerical simulations.

For long times, the progression of the mean concentration distribution with an instantaneous central point source release is shown in figure 13. The long-tailed distribution is rather persistent as the distribution proceeds to approach a more symmetric Gaussian-type shape. The fourth-order solution gives reasonable approximations of the mean concentration as verified by the numerical results. It also considerably outweighs the long-time asymptotic expansions of Chatwin (1970) and Gill *et al.* (1970), especially before the classical Taylor dispersion regime.

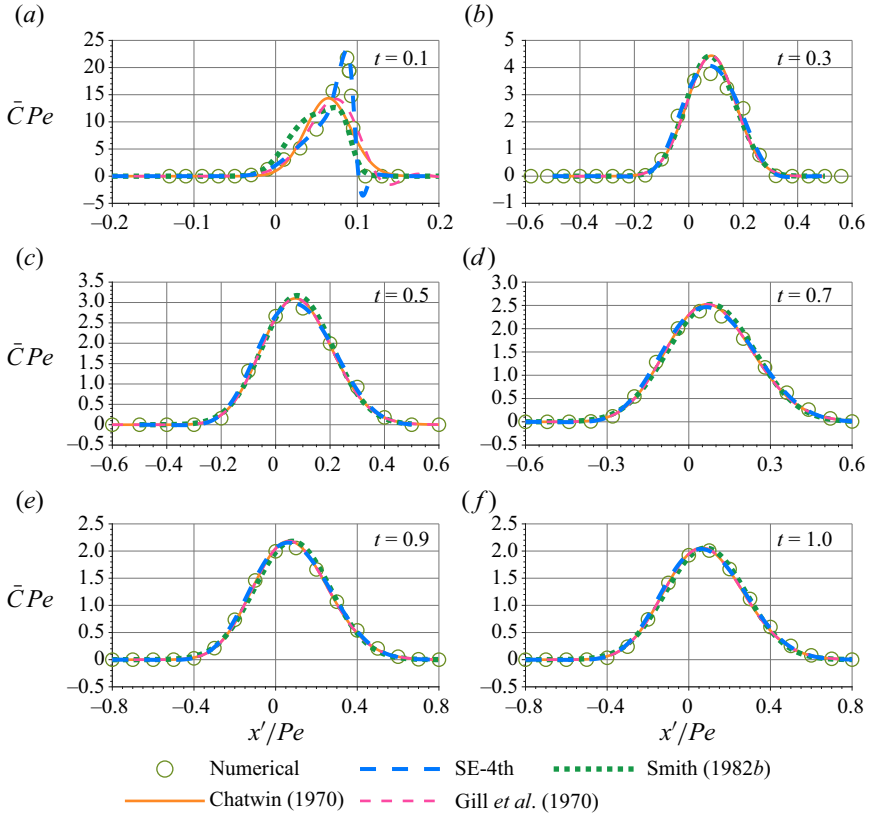

Figure 13. Axial distributions of mean concentration at long times obtained by Smith (1982*b*), Chatwin (1970), Gill *et al.* (1970) and the present (fourth-order) streamwise expansion compared to the numerical results. Common parameters are $Pe = 10\,000$ and $r_0 = 0$.

Figure 14 compares the concentration contours as predicted by the analytical solution with the full numerical solution of the convection–diffusion equation. Besides the remarkable non-uniform features, exact concentration profiles also show concentration peaks on the axis in figure 14(*a*) and near the boundary wall in figure 14(*b*). Compared to the area source, the basic origins of the asymmetrical structures are attached to the initial non-uniformity apart from shear distortion and the effect of boundary walls. The non-uniform features have been reproduced reasonably, and the peaks at the walls are also predicted quantitatively. Peculiar island-shaped structures of the transverse concentration from a central point source are revealed in figures 14(*a–c*), during the pre-asymptotic regime. On the whole, the present streamwise dispersion model captures the physical structures, temporal evolution of two-dimensional and mean concentration distribution, corroborated satisfactorily by the numerical simulations.

Finally, it is worthwhile to clarify the relations between the present streamwise expansions and some well-known asymptotic expansions. Chatwin's long-time approximation is equivalent to the Edgeworth expansion for infinitely long times. Besides, the Gram–Charlie type A series adopted by Smith (1982*b*) is not a true asymptotic expansion regarding concentration distribution governed by the convection–diffusion equation. It is noteworthy that Gill's unsteady dispersion model embodies the form of Chatwin's steady dispersion model, by equating the time-dependent coefficients to the limits of $t \to \infty$ with the loss of superposable properties. These infinite series differ

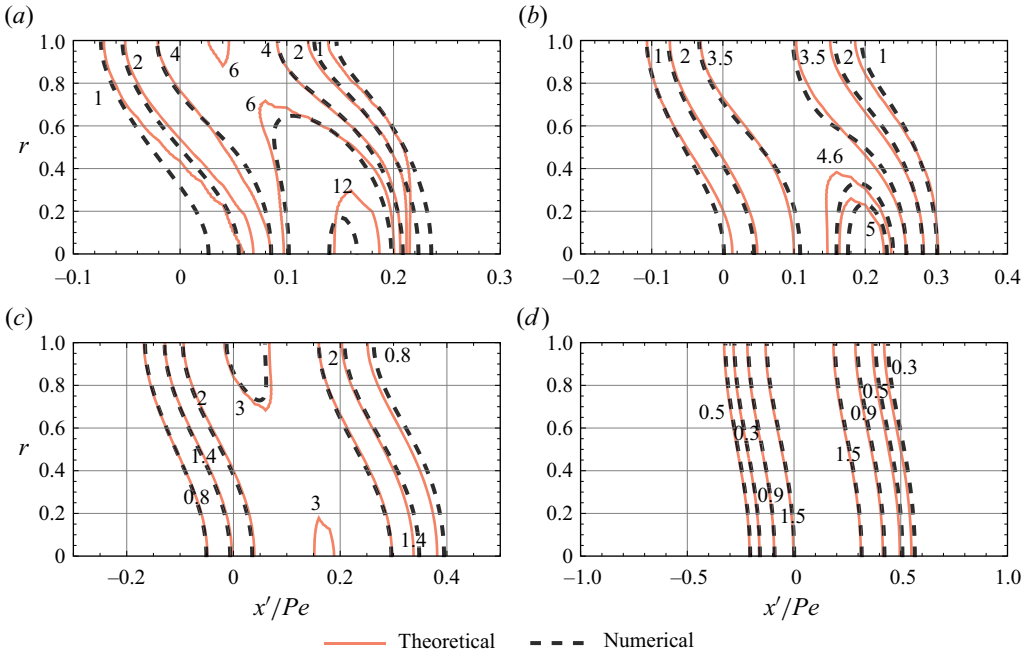

Figure 14. Contours of azimuthally averaged concentration distribution from a central point source for $Pe = 10\,000$ obtained by the present (fourth-order) streamwise expansion compared to the numerical results.

eventually because of finite truncation techniques. Also, the present choice of streamwise expansion outweighs other long-time expansions for both the fundamental point and area sources, which best captures the long-tail hallmark, skewed platforms, and peculiar island-shaped structures with the central point discharge during the transitional regimes. The generalisation of the existing dispersion models is analysed in detail in § 4 of the supplementary material.

In summary, the analytical solutions of the developed streamwise dispersion model asymptotes to Taylor's well-known dispersion results for long times, whereas the components of the equivalent diffusivity tensor are nonlinear and anisotropic functions of time and space coordinates. Our generalisation lies in incorporating the local corrections of spatial concentration moments other than mean concentration moments, and Edgeworth modifications to determine the coefficients of comparable magnitude, with the understanding that the interchange of averaging operation and differential operator make remarkable differences. Since this spirit comes from first principles, it could have wide adaptability to the exiting dispersion models (Chatwin 1970; Gill *et al.* 1970; Frankel & Brenner 1989) and generalised transport problem (Christov & Stone 2012; Golestanian 2012; Masoud & Stone 2019; Morris 2020; Zeng, Jiang & Pedley 2022), including diffusion of granular materials, heat transfer, and pre-asymptotic active dispersion of active colloids and micro-organisms.

6. Concluding remarks

The above sections present a novel streamwise theory of dispersion based on a convection transformation from a Lagrangian perspective. In particular, (3.22) gives a diffusion-type formulation of streamwise dispersion that revives appreciable Taylor

dispersion results and yields a short-time particular solution. This theory allows, for the first time, a unified conceptualisation of the whole dispersive spreading of soluble matter from initial to dispersion regimes. The short-time benchmark, complementary to the well-known Taylor–Aris solution, is capable of essential statistical–physical features of mean concentration, e.g. unique heads and tails of concentration profiles, when the flow convection dominates over molecular diffusion. Analytical results are well corroborated by Monte Carlo simulations.

The convectively transformed governing equation deduces naturally three time scales with respect to the Péclet number, lending the ground for the derivation of the streamwise dispersion model. With particular solutions in hand for both asymptotically short and long times, a streamwise dispersion model is devised by series expansions of concentration statistics in local moment space. Analytical solutions are given for the typical area and point sources in the classical Poiseuille flow. These solutions reveal richer physical structures, including persistent long tails and skewed platforms, and collaborate in good agreement with numerical results of the transverse and mean concentration from the initial release to the Taylor dispersion regime. The fact that solutions of the truncated streamwise dispersion model asymptote to the limiting particular solutions, wedded to the fact that this moment-based expansion contains precise streamwise information, implies that the nature of dispersion is exactly superposable diffusion-type processes, corresponding to components of diffusivity tensor anisotropic in space and nonlinear with time; compare (3.19).

It should be noted, however, that the prevalent deduction that Hermite series approximation of the transport of a solute fails to reproduce accurately the averaged concentration profiles over the cross-section (Chatwin 1970; Smith 1982*b*) has not been gratuitous. Although the previous results give qualitative hallmarks of mean concentration, characteristic asymmetric results could not be obtained with the existing dispersion models due to the limited truncated order and inexact cross-sectional statistics. Moreover, the coarse-grained Taylor–Aris framework could hardly induce further useful conceptual insights into the overall macro-scale transport process comprised of micro-scale advective and diffusive (i.e. dispersion) mechanisms for its very limited or even abused knowledge of streamwise information. In the light of streamwise theory of dispersion, combined with Edgeworth modification in statistical theory introduced to collect terms of comparable magnitude, our analytical solution of the developed streamwise dispersion model gives remarkably accurate predictions for the cases from typical point and area sources. We emphasise that comparable insights would hardly be derived from pure numerical simulations. As a unified analytical model capable of featuring the overall dispersion process, the physical elucidation of streamwise dispersivity, transverse concentration and their mean over the cross-section clearly contribute essential physical insights into the global perspective of related transport processes.

The new contribution asserts that a streamwise perspective could better depict the peculiar peaks in the instantaneous change of streamwise dispersion and asymmetric collective behaviour of soluble matter. The characteristic peak of streamwise dispersivity perceptibly beyond the long-time Taylor–Aris limit, corresponding to the right-skewed platforms of mean concentration, shows a greatly enhanced dispersion of the solute during the pre-asymptotic regime. From the fundamental level of marginal density distribution, the motion not only could be understood mathematically as from the delay of relaxation time between the first and second moments, but also appeals to physical explanations from the classical continuum–mechanical perspective as the effect of non-penetration boundary sets when the tracer is dispersed under the combined action of streamwise convection and transverse molecular diffusion. The peculiar phenomenon is present only for point

sources released relatively near the central axis, whence the soluble matter is able to cross streamlines from high to low shear through molecular diffusion before approaching the wall.

Given the fact that there is no analytical solution of the convection–diffusion problem, it is natural to inquire how to predict the asymptotic motion of soluble matter in a concise framework. This important problem was explored originally by Taylor (1953) and Aris (1956) more than half a century ago, resulting in the well-known Taylor–Aris dispersion theory. Inputting the constant mean drift $\bar{\Phi}_T(\infty)$ and dispersivity $\bar{D}_T(\infty)$, one is able to output precisely the mean concentration $\bar{C}$ for asymptotically long times. To pursue a more conceptually insightful paradigm for the overall dispersion process, a unified description of transient dispersion is desirable yet elusive to date. The convection–diffusion equation of concentration (3.1) constitutes an Eulerian description of transport of soluble matter in the form of marginal probability distribution (5.1). It would be beneficial to explain why the transient dispersion results are non-trivial and indeed heuristic, alternatively from a Lagrangian view as (3.22). Physically, the drift velocity represents the axial displacement of the cloud of soluble matter along each streamline. In a moving system at the speed of mean flow velocity, Taylor's first relation $\bar{\Phi}_T(\infty) \sim 0$ corresponds to the identity of mean solute and solvent velocities. This result is non-trivial in that it is an equality of the Eulerian solvent velocity and Lagrangian solute velocity. As shown in the pre-asymptotic regime, the general case would have inequality of these two quantities, of which the differences give rise to interesting phenomena of peculiar characteristic peaks and asymmetric concentration profiles.

Taylor's celebrated second relation $\bar{D}_T(\infty) \sim (1 + Pe^2/48)t$ is more appreciable, by analogy of Einstein's well-known Brownian diffusion relation for a quiescent fluid. In contrast, the dispersion relation is true asymptotically only after the tracer has sampled each streamline with equal opportunities through the whole cross-section. Once again, this is non-trivial since the second term of this relation constitutes a remarkable yet nonlinear contribution of enhanced axial diffusion, arising from axial convection and lateral Brownian motion. With the streamwise dispersion theory, we show that transverse positions of the soluble matter across the tube indeed do not 'attract' the solute molecule equally. The effects of flow convection and reflective boundary indeed attenuate the transverse diffusion, and could result in a significantly enhanced axial spreading even exceeding the Taylor–Aris limit. Furthermore, we show that the overall Taylor–Aris dispersivity is instead a fictitious quantity of the whole cloud of soluble matter, which is definitionally valid only for asymptotically long times. We emphasise that only the streamwise dispersivity captures exactly the axial displacement along each streamline and exhibits clearly the remarkable enhancement of axial spreading, although both definitions of dispersivity asymptote to the same constant in the long-time limit.

The developed theory and obtained results are heuristic to reveal the physical structures of concentration distributions. For a central point release, we show that a tilted Gaussian distribution of concentration appears long before a paraboloidal snout is pulled out by tube flows, then skews when colliding with the wall, and eventually disperses into a steady state. Peculiar peaks of streamwise dispersivity, island-shaped structures and asymmetric skewed platforms of the concentration distribution depict consistently the non-equilibrium state of dispersion. The influences of initial conditions, shear distortion, cross-enhancement and boundary effects on the asymmetric features of concentration distribution are illustrated and elaborated. The right-skewed platform of transverse concentration and peculiar characteristic peaks of streamwise dispersivity are highlighted as hallmarks of the transient dispersion of a solute. This phenomenon corresponding to a

greatly enhanced effective diffusivity could shed new light on the mixing and dispersion of various passive and active matter. It would also be interesting to see if this theoretical prediction is borne out in experiments.

As a last remark, the key idea behind this novel streamwise theory of dispersion is a unified combination of Lagrangian and Eulerian views. The equivalent diffusivity tensor includes three components distinctively for isotropic molecular diffusion ($\boldsymbol{D}^{(\boldsymbol{O})}$), a cross-enhancement due to shear of the external velocity field ($\boldsymbol{D}^{(\boldsymbol{C})}$), and a dispersal enhancement only along the streamwise direction ($\boldsymbol{D}^{(\boldsymbol{E})}$). This partition with respect to three time scales (in each order of $Pe\,t$) shows that the components are anisotropic in space and nonlinear with time, and also confirms the developed model and solutions. To better understand the implications of the physical structures, we resort to the diffusion flux vector and give a short-cut picture of how a solute is distorted in a tube flow. Further, it is certified that the persistent asymmetries of concentration distribution through a circular tube have basically at least three origins: (*a*) initial non-uniformity, (*b*) unidirectional convective distortion, and (*c*) zero-flux effect of wall boundary. Generically, the formulation presented in the streamwise theory of dispersion allows one to investigate properly the transient dispersion of passive (and active) particles in rich flow conditions under the combined action of flow convection and diffusion (whose origin could be athermal), and is open to include fundamental factors, including particle anisotropy, active swimming and finite size. We expect that this new streamwise perspective could advance our understanding of macro-transport processes widely for both passive solutes and active micro-swimmers.

Supplementary material. Supplementary material is available at https://doi.org/10.1017/jfm.2024.34.

Acknowledgements. The authors extend sincere thanks to Professors Luoyi Tao, Zhi Li and Weiquan Jiang, and anonymous referees for their constructive comments.

Funding. This work is supported by the National Natural Science Foundation of China (grant nos 12372379 and 52079001).

Declaration of interests. The authors report no conflict of interest.

Author ORCIDs.
Mingyang Guan https://orcid.org/0000-0001-5341-7561;
Guoqian Chen https://orcid.org/0000-0003-1173-6796.

References

Abbott, M.R., Denman, K.L., Powell, T.M., Richerson, P.J., Richards, R.C. & Goldman, C.R. 1984 Mixing and the dynamics of the deep chlorophyll maximum in Lake Tahoe. *Limnol. Oceanogr.* **29** (4), 862–878.

Alessio, B.M., Shim, S., Gupta, A. & Stone, H.A. 2022 Diffusioosmosis-driven dispersion of colloids: a Taylor dispersion analysis with experimental validation. *J. Fluid Mech.* **942**, A23.

Aris, R. 1956 On the dispersion of a solute in a fluid flowing through a tube. *Proc. R. Soc. Lond.* A **235** (1200), 67–77.

Barry, M.T., Rusconi, R., Guasto, J.S. & Stocker, R. 2015 Shear-induced orientational dynamics and spatial heterogeneity in suspensions of motile phytoplankton. *J. R. Soc. Interface* **12** (112), 20150791.

Bearon, R.N. & Hazel, A.L. 2015 The trapping in high-shear regions of slender bacteria undergoing chemotaxis in a channel. *J. Fluid Mech.* **771**, R3.

Bearon, R.N., Hazel, A.L. & Thorn, G.J. 2011 The spatial distribution of gyrotactic swimming micro-organisms in laminar flow fields. *J. Fluid Mech.* **680**, 602–635.

Bello, M.S., Rezzonico, R. & Righetti, P.G. 1994 Use of Taylor–Aris dispersion for measurement of a solute diffusion coefficient in thin capillaries. *Science* **266** (5186), 773–776.

Biswas, R.R. & Sen, P.N. 2007 Taylor dispersion with absorbing boundaries: a stochastic approach. *Phys. Rev. Lett.* **98** (16), 164501.

BRENNER, H. & EDWARDS, D. 1993 *Macrotransport Processes*. Butterworth-Heinemann.
CHATWIN, P.C. 1970 The approach to normality of the concentration distribution of a solute in a solvent flowing along a straight pipe. *J. Fluid Mech.* **43** (2), 321–352.
CHATWIN, P.C. 1972 The cumulants of the distribution of concentration of a solute dispersing in solvent flowing through a tube. *J. Fluid Mech.* **51** (1), 63–67.
CHATWIN, P.C. 1974 The dispersion of contaminant released from instantaneous sources in laminar flow near stagnation points. *J. Fluid Mech.* **66** (4), 753–766.
CHATWIN, P.C. 1976 The initial dispersion of contaminant in Poiseuille flow and the smoothing of the snout. *J. Fluid Mech.* **77** (3), 593–602.
CHATWIN, P.C. 1977 The initial development of longitudinal dispersion in straight tubes. *J. Fluid Mech.* **80** (1), 33–48.
CHATWIN, P.C. & ALLEN, C.M. 1985 Mathematical models of dispersion in rivers and estuaries. *Annu. Rev. Fluid Mech.* **17**, 119–149.
CHEN, G. & GAO, Z. 1991 A transformation of the convective diffusion equation with corresponding finite difference method. *Chin. J. Theor. Appl. Mech.* **23** (4), 418–425.
CHEN, G.Q., GAO, Z. & YANG, Z.F. 1993 A perturbational h^4 exponential finite difference scheme for the convective diffusion equation. *J. Comput. Phys.* **104** (1), 129–139.
CHIKWENDU, S.C. 1986 Calculation of longitudinal shear dispersivity using an N-zone model as $N \to \infty$. *J. Fluid Mech.* **167**, 19–30.
CHIKWENDU, S.C. & OJIAKOR, G.U. 1985 Slow-zone model for longitudinal dispersion in two-dimensional shear flows. *J. Fluid Mech.* **152**, 15–38.
CHRISTOV, I.C. & STONE, H.A. 2012 Resolving a paradox of anomalous scalings in the diffusion of granular materials. *Proc. Natl Acad. Sci. USA* **109** (40), 16012–16017.
CHU, H.C.W., GAROFF, S., TILTON, R.D. & KHAIR, A.S. 2021 Macrotransport theory for diffusiophoretic colloids and chemotactic microorganisms. *J. Fluid Mech.* **917**, A52.
CRANK, J. 1975 *The Mathematics of Diffusion*, 2nd edn. Clarendon Press.
DEBNATH, S., JIANG, W., GUAN, M. & CHEN, G. 2022 Effect of ring-source release on dispersion process in Poiseuille flow with wall absorption. *Phys. Fluids* **34** (2), 027106.
DELEANU, M., HERNANDEZ, J.-F., CIPELLETTI, L., BIRON, J.-P., ROSSI, E., TAVERNA, M., COTTET, H. & CHAMIEH, J. 2021 Unraveling the speciation of β-amyloid peptides during the aggregation process by Taylor dispersion analysis. *Anal. Chem.* **93** (16), 6523–6533.
DEWEY, R.J. & SULLIVAN, P.J. 1982 Longitudinal-dispersion calculations in laminar flows by statistical analysis of molecular motions. *J. Fluid Mech.* **125**, 203–217.
DURHAM, W.M., CLIMENT, E., BARRY, M., DE LILLO, F., BOFFETTA, G., CENCINI, M. & STOCKER, R. 2013 Turbulence drives microscale patches of motile phytoplankton. *Nat. Commun.* **4** (1), 2148.
DURHAM, W.M., KESSLER, J.O. & STOCKER, R. 2009 Disruption of vertical motility by shear triggers formation of thin phytoplankton layers. *Science* **323** (5917), 1067–1070.
ELDER, J.W. 1959 The dispersion of marked fluid in turbulent shear flow. *J. Fluid Mech.* **5** (4), 544–560.
EZHILAN, B. & SAINTILLAN, D. 2015 Transport of a dilute active suspension in pressure-driven channel flow. *J. Fluid Mech.* **777**, 482–522.
FALLON, M.S., HOWELL, B.A. & CHAUHAN, A. 2009 Importance of Taylor dispersion in pharmacokinetic and multiple indicator dilution modelling. *Math. Med. Biol.* **26** (4), 263–296.
FISCHER, H.B. 1972 Mass transport mechanisms in partially stratified estuaries. *J. Fluid Mech.* **53**, 671–687.
FISCHER, H.B. 1973 Longitudinal dispersion and turbulent mixing in open-channel flow. *Annu. Rev. Fluid Mech.* **5** (1), 59–78.
FISCHER, H.B. 1976 Mixing and dispersion in estuaries. *Annu. Rev. Fluid Mech.* **8** (1), 107–133.
FISCHER, H.B. (Ed.) 1979 *Mixing in Inland and Coastal Waters*. Academic Press.
FOISTER, R.T. & VAN DE VEN, T.G.M. 1980 Diffusion of Brownian particles in shear flows. *J. Fluid Mech.* **96** (1), 105–132.
FRANKEL, I. & BRENNER, H. 1989 On the foundations of generalized Taylor dispersion theory. *J. Fluid Mech.* **204**, 97–119.
FUNG, L., BEARON, R.N. & HWANG, Y. 2022 A local approximation model for macroscale transport of biased active Brownian particles in a flowing suspension. *J. Fluid Mech.* **935**, A24.
GEKLE, S. 2017 Dispersion of solute released from a sphere flowing in a microchannel. *J. Fluid Mech.* **819**, 104–120.
GILL, W. 1971 Dispersion of a non-uniform slug in time-dependent flow. *Proc. R. Soc. Lond.* A **322** (1548), 101–117.
GILL, W.N. 1967 A note on the solution of transient dispersion problems. *Proc. R. Soc. Lond.* A **298** (1454), 335–339.

GILL, W.N., SANKARASUBRAMANIAN, R. & TAYLOR, G.I. 1970 Exact analysis of unsteady convective diffusion. *Proc. R. Soc. Lond.* A **316** (1526), 341–350.
GOLESTANIAN, R. 2012 Collective behavior of thermally active colloids. *Phys. Rev. Lett.* **108** (3), 038303.
GUAN, M., JIANG, W., WANG, B., ZENG, L., LI, Z. & CHEN, G. 2023 Pre-asymptotic dispersion of active particles through a vertical pipe: the origin of hydrodynamic focusing. *J. Fluid Mech.* **962**, A14.
GUAN, M., ZENG, L., JIANG, W., GUO, X., WANG, P., WU, Z., LI, Z. & CHEN, G. 2022 Effects of wind on transient dispersion of active particles in a free-surface wetland flow. *Commun. Nonlinear Sci. Numer. Simul.* **115**, 106766.
GUAN, M., ZENG, L., LI, C., GUO, X., WU, Y. & WANG, P. 2021 Transport model of active particles in a tidal wetland flow. *J. Hydrol.* **593**, 125812.
GUO, J. & CHEN, G. 2022 Solute dispersion from a continuous release source in a vegetated flow: an analytical study. *Water Resour. Res.* **58**, e2021WR030255.
GUO, J., JIANG, W. & CHEN, G. 2020 Transient solute dispersion in wetland flows with submerged vegetation: an analytical study in terms of time-dependent properties. *Water Resour. Res.* **56** (2), e2019WR025586.
HABER, S. & MAURI, R. 1988 Lagrangian approach to time-dependent laminar dispersion in rectangular conduits. Part 1. Two-dimensional flows. *J. Fluid Mech.* **190**, 201–215.
HAHN, D.W. & ÖZIŞIK, M.N. 2012 *Heat Conduction*. John Wiley & Sons.
HONG, J., WU, H., ZHANG, R., HE, M. & XU, W. 2020 The coupling of Taylor dispersion analysis and mass spectrometry to differentiate protein conformations. *Anal. Chem.* **92** (7), 5200–5206.
HOUSEWORTH, J.E. 1984 Shear dispersion and residence time for laminar flow in capillary tubes. *J. Fluid Mech.* **142**, 289–308.
JIANG, W. & CHEN, G. 2018 Solution of Gill's generalized dispersion model: solute transport in Poiseuille flow with wall absorption. *Intl J. Heat Mass Transfer* **127**, 34–43.
JIANG, W. & CHEN, G. 2019 Dispersion of active particles in confined unidirectional flows. *J. Fluid Mech.* **877**, 1–34.
JIANG, W. & CHEN, G. 2021 Transient dispersion process of active particles. *J. Fluid Mech.* **927**, A11.
JIANG, W., ZENG, L., FU, X. & WU, Z. 2022 Analytical solutions for reactive shear dispersion with boundary adsorption and desorption. *J. Fluid Mech.* **947**, A37.
KENDALL, M.G. & STUART, A. 1958 *The Advanced Theory of Statistics*, vol. 1. Griffin.
KESSLER, J.O. 1985 Hydrodynamic focusing of motile algal cells. *Nature* **313** (5999), 218–220.
LATINI, M. & BERNOFF, A.J. 2001 Transient anomalous diffusion in Poiseuille flow. *J. Fluid Mech.* **441**, 399–411.
LI, G. 2018 An extended Taylor–Aris method in dispersion theory and its applications. PhD thesis, Peking University.
LI, G. & TANG, J.X. 2009 Accumulation of microswimmers near a surface mediated by collision and rotational Brownian motion. *Phys. Rev. Lett.* **103** (7), 078101.
LIGHTHILL, M.J. 1966 Initial development of diffusion in Poiseuille flow. *J. Inst. Maths Applics.* **2**, 97–108.
MASOUD, H. & STONE, H.A. 2019 The reciprocal theorem in fluid dynamics and transport phenomena. *J. Fluid Mech.* **879**, P1.
MERCER, G.N. & ROBERTS, A.J. 1990 A centre manifold description of contaminant dispersion in channels with varying flow properties. *SIAM J. Appl. Maths* **50** (6), 1547–1565.
MERCER, G.N. & ROBERTS, A.J. 1994 A complete model of shear dispersion in pipes. *Japan J. Ind. Appl. Maths* **11** (3), 499.
MORRIS, J.F. 2020 Shear thickening of concentrated suspensions: recent developments and relation to other phenomena. *Annu. Rev. Fluid Mech.* **52** (1), 121–144.
MOSER, M.R. & BAKER, C.A. 2021 Taylor dispersion analysis in fused silica capillaries: a tutorial review. *Anal. Methods* **13** (21), 2357–2373.
NAKAD, M., WITELSKI, T., DOMEC, J.C., SEVANTO, S. & KATUL, G. 2021 Taylor dispersion in osmotically driven laminar flows in phloem. *J. Fluid Mech.* **913**, A44.
PASMANTER, R.A. 1985 Exact and approximate solutions of the convection–diffusion equation. *Q. J. Mech. Appl. Maths* **38** (1), 1–26.
PEDLEY, T.J. & KESSLER, J.O. 1992 Hydrodynamic phenomena in suspensions of swimming microorganisms. *Annu. Rev. Fluid Mech.* **24** (1), 313–358.
PHILLIPS, C.G. & KAYE, S.R. 1997 The initial transient of concentration during the development of Taylor dispersion. *Proc. R. Soc. Lond.* A **453** (1967), 2669–2688.
RUSCONI, R., GUASTO, J.S. & STOCKER, R. 2014 Bacterial transport suppressed by fluid shear. *Nat. Phys.* **10** (3), 212–217.
SAFFMAN, P.G. 1960 On the effect of the molecular diffusivity in turbulent diffusion. *J. Fluid Mech.* **8** (2), 273–283.
SMITH, R. 1981 A delay-diffusion description for contaminant dispersion. *J. Fluid Mech.* **105**, 469–486.

SMITH, R. 1982*a* Contaminant dispersion in oscillatory flows. *J. Fluid Mech.* **114** (-1), 379.
SMITH, R. 1982*b* Gaussian approximation for contaminant dispersion. *Q. J. Mech. Appl. Maths* **35** (3), 345–366.
SOKOLOV, A. & ARANSON, I.S. 2016 Rapid expulsion of microswimmers by a vortical flow. *Nat. Commun.* **7**, 11114.
STOKES, A.N. & BARTON, N.G. 1990 The concentration distribution produced by shear dispersion of solute in Poiseuille flow. *J. Fluid Mech.* **210**, 201–221.
SULLIVAN, P.J. 1971 Longitudinal dispersion within a two-dimensional turbulent shear flow. *J. Fluid Mech.* **49** (3), 551–576.
TAGHIZADEH, E., VALDÉS-PARADA, F.J. & WOOD, B.D. 2020 Preasymptotic Taylor dispersion: evolution from the initial condition. *J. Fluid Mech.* **889**, A5.
TAYLOR, G.I. 1953 Dispersion of soluble matter in solvent flowing slowly through a tube. *Proc. R. Soc. Lond.* A **219** (1137), 186–203.
TAYLOR, G.I. 1954*a* Conditions under which dispersion of a solute in a stream of solvent can be used to measure molecular diffusion. *Proc. R. Soc. Lond.* A **225** (1163), 473–477.
TAYLOR, G.I. 1954*b* Diffusion and mass transport in tubes. *Proc. Phys. Soc.* B **67** (12), 857.
TAYLOR, G.I. 1954*c* The dispersion of matter in turbulent flow through a pipe. *Proc. R. Soc. Lond.* A **223** (1155), 446–468.
TAYLOR, G.I. 1959 The present position in the theory of turbulent diffusion. *Adv. Geophys.* **6**, 101–112.
TOWNSEND, A.A. & TAYLOR, G.I. 1951 The diffusion of heat spots in isotropic turbulence. *Proc. R. Soc. Lond.* A **209** (1098), 418–430.
VEDEL, S. & BRUUS, H. 2012 Transient Taylor–Aris dispersion for time-dependent flows in straight channels. *J. Fluid Mech.* **691**, 95–122.
VEDEL, S., HOVAD, E. & BRUUS, H. 2014 Time-dependent Taylor–Aris dispersion of an initial point concentration. *J. Fluid Mech.* **752**, 107–122.
VILQUIN, A., BERTIN, V., RAPHAËL, E., DEAN, D.S., SALEZ, T. & MCGRAW, J.D. 2023 Nanoparticle Taylor dispersion near charged surfaces with an open boundary. *Phys. Rev. Lett.* **130** (3), 038201.
WANG, B., JIANG, W. & CHEN, G. 2022*a* Gyrotactic trapping of micro-swimmers in simple shear flows: a study directly from the fundamental Smoluchowski equation. *J. Fluid Mech.* **939**, A37.
WANG, B., JIANG, W. & CHEN, G. 2023 Dispersion of a gyrotactic micro-organism suspension in a vertical pipe: the buoyancy–flow coupling effect. *J. Fluid Mech.* **962**, A39.
WANG, B., JIANG, W., CHEN, G. & TAO, L. 2022*b* Transient dispersion in a channel with crossflow and wall adsorption. *Phys. Rev. Fluids* **7** (7), 074501.
WANG, P. & CHEN, G. 2016*a* Transverse concentration distribution in Taylor dispersion: Gill's method of series expansion supported by concentration moments. *Intl J. Heat Mass Transfer* **95**, 131–141.
WANG, P. & CHEN, G.Q. 2016*b* Solute dispersion in open channel flow with bed absorption. *J. Hydrol.* **543**, 208–217.
WANG, P. & CHEN, G. 2017 Basic characteristics of Taylor dispersion in a laminar tube flow with wall absorption: exchange rate, advection velocity, dispersivity, skewness and kurtosis in their full time dependance. *Intl J. Heat Mass Transfer* **109**, 844–852.
WANG, P. & CIRPKA, O.A. 2021 Surface transient storage under low-flow conditions in streams with rough bathymetry. *Water Resour. Res.* **57** (12), e2021WR029899.
WU, Z. & CHEN, G. 2014 Approach to transverse uniformity of concentration distribution of a solute in a solvent flowing along a straight pipe. *J. Fluid Mech.* **740**, 196–213.
WU, Z., FURBISH, D. & FOUFOULA-GEORGIOU, E. 2020 Generalization of hop distance-time scaling and particle velocity distributions via a two-regime formalism of bedload particle motions. *Water Resour. Res.* **56** (1), e2019WR025116.
WU, Z., JIANG, W., ZENG, L. & FU, X. 2023 Theoretical analysis for bedload particle deposition and hop statistics. *J. Fluid Mech.* **954**, A11.
YASA, O., ERKOC, P., ALAPAN, Y. & SITTI, M. 2018 Microalga-powered microswimmers toward active cargo delivery. *Adv. Mater.* **30** (45), 1804130.
YASUDA, H. 1984 Longitudinal dispersion of matter due to the shear effect of steady and oscillatory currents. *J. Fluid Mech.* **148**, 383–403.
YOUNG, W.R. & JONES, S. 1991 Shear dispersion. *Phys. Fluids* **3** (5), 1087–1101.
ZENG, L., JIANG, W. & PEDLEY, T.J. 2022 Sharp turns and gyrotaxis modulate surface accumulation of microorganisms. *Proc. Natl Acad. Sci. USA* **119** (42), e2206738119.
ZHANG, L., HESSE, M.A. & WANG, M. 2017 Transient solute transport with sorption in Poiseuille flow. *J. Fluid Mech.* **828**, 733–752.